

Accelerating FRB Search: Dataset and Methods

XUERONG GUO,¹ YINAN KE,¹ YIFAN XIAO,¹ HUAXI CHEN,¹ CHENCHEN MIAO,¹ PEI WANG,² DI LI,² HAN WANG,¹
CHENWU JIN,¹ LING HE,¹ YI FENG,¹ YONGKUN ZHANG,² JIAYING XU,¹ AND GUANGYONG CHEN¹

¹Zhejiang Lab

²National Astronomical Observatories

ABSTRACT

Fast Radio Burst (FRB) is an extremely energetic cosmic phenomenon of short duration. Discovered only recently and with yet unknown origin, FRBs have already started to play a significant role in studying the distribution and evolution of matter in the universe. FRBs can only be observed through radio telescopes, which produce petabytes of data, rendering the search for FRB a challenging task. Traditional techniques are computationally expensive, time-consuming, and generally biased against weak signals. Various machine learning algorithms have been developed and employed, which all require substantial data sets. We here introduce the FAST dataset for Fast Radio bursts EXploration (FAST-FREX), built upon the observations obtained by the Five-hundred-meter Aperture Spherical radio Telescope (FAST). Our dataset comprises 600 positive samples of observed FRB signals from three sources and 1000 negative samples of noise and Radio Frequency Interference (RFI). Furthermore, we provide a machine learning algorithm, Radio Single-Pulse Detection Algorithm Based on Visual Morphological Features (RaSPDAM), with significant improvements in efficiency and accuracy for FRB search. We also employed the benchmark comparison between conventional single-pulse search softwares, namely PRESTO and Heimdall, and RaSPDAM. Future machine learning algorithms can use this as a reference point to measure their performance and help the potential improvements.

Keywords: Fast radio bursts(2008) — Astronomy databases(83) — Astronomy software(1855)

1. INTRODUCTION

Fast Radio Burst (FRB) is a rapidly developing field in astrophysics that researchers extensively explore regarding its origin, emission mechanisms, and applications. FRBs are characterized by their short duration, high-energy release, and widespread distribution in the universe, which is crucial in studying the distribution and evolution of matter in the cosmos. Despite the discovery of about a few hundred FRBs (Li et al. 2021; Niu et al. 2022a; Feng et al. 2022; Zhang et al. 2022), their origin and physical mechanisms are still a mystery. The discovery of more FRBs is expected to bring revolutionary breakthroughs in physics and astronomy.

Various open-source software packages have been developed for searching single-pulse signals to discover FRBs, long-period pulsars, and other radio transient sources. PRESTO (Ransom 2011) and SIGPROC (Lorimer 2011) are two software packages designed to standardize the initial analysis of various fast-sampled pulsar data types and have aided in the discovery of numerous pulsar

radio sources. Heimdall¹, a single-pulse search algorithm based on Graphical Processing Units (GPUs), can enhance data processing efficiency to a certain degree. These software packages' pipelines usually employ computation-intensive dispersion removal algorithms on search data, producing several time sequences with dispersion effects removed, which might lead to significant computational time. On the other hand, Radio Frequency Interference (RFI) and instrument noise make detecting weaker pulse signals challenging.

In recent years, the field of astronomy has extensively applied machine learning methods, providing novel approaches and more efficient practical methods for detecting FRBs. Based on deep learning classifiers, these methods can effectively reduce the substantial number of false-positive single-pulse candidates, mainly due to RFI (Agarwal et al. 2020b,a; Connor & van Leeuwen 2018; Chen et al. 2023). The above methods rely on FRB candidates generated from single-pulse search algorithms

¹ <https://sourceforge.net/p/heimdall-astro/wiki/Home/>

that use de-dispersion. The current FRB detector directly analyses raw observational data (Liu et al. 2022). These algorithms can process search data in real-time and detect weak signals that current search technologies might have missed. However, training machine learning models requires a substantial amount of data samples. Consequently, supplying a FRB dataset for the machine learning algorithm research is an impending issue that needs to be resolved urgently.

Astronomical telescopes have gathered extensive observational data that aids in the search for FRBs. The Chinese Five-hundred-meter Aperture Spherical radio Telescope (FAST) (Li et al. 2018; Jiang et al. 2019), which is the world’s biggest single-aperture telescope with the highest sensitivity, can detect weak signals that other radio telescopes cannot detect due to its precise surface reflection control and the favorable polarization characteristics of its FAST-19 beam receiver. The research team utilized FAST to detect 1652 outbursts in about a 50-day interval through the Commensal Radio Astronomy FAST Survey (CRAFTS), obtaining the most extensive sample of FRB outbursts to date and revealing the complete spectrum and bimodal structure of the burst rate for the first time (Li et al. 2021).

This paper proposes the FAST dataset for Fast Radio bursts EXploration (FAST-FREX). FAST-FREX was derived from the authentic observation data obtained from FAST, containing FRB signals from multiple sources. The FRB sources include FRB20121102 (Li et al. 2021), FRB20180301 (Laha et al. 2022) and FRB20201124 (Zhang et al. 2022; Niu et al. 2022b). FAST-FREX aims to facilitate the advancement of machine learning algorithms for FRB search, enabling the exploration of more FRB events. We introduce a machine learning algorithm, Radio Single-Pulse Detection Algorithm Based on Visual Morphological Features (RaSPDAM), showcasing substantial improvements in efficiency and accuracy on FRB search. Furthermore, we present the benchmark results from two conventional softwares and RaSPDAM, serving as baselines for evaluating the performance of machine learning algorithms in future research.

The paper is structured as follows: Section 2 outlines the present state of dataset construction in the astronomy field. Section 3 details the methods and parameter specifications employed to create the dataset. Section 4 comprehensively explains the machine learning algorithm RaSPDAM and introduces two conventional search software, PRESTO and Heimdall. The benchmark results of these methods are presented in Section 5 as the baselines. Section 6 introduces the application of the algorithm RaSPDAM and the pulsars discovered by

the algorithm. Section 7 highlights the limitations of the dataset and potential challenges. Finally, Section 8 presents the conclusion and outlines future directions.

2. RELATED WORK

At present, astronomical data is primarily obtained from multiple telescopes that record data according to their specific standards, resulting in a lack of uniformity. Additionally, observational targets and recording patterns differ based on the research field. Some open-source datasets are available for pulsar, and FRB searches to address this issue.

The HTRU2 dataset (Lyon et al. 2016), which stems from The High Time Resolution Universe Pulsar Survey project (Keith et al. 2010), comprises a significant number of pulsar candidates, totaling 17,898 samples. The sample set consists of 1,639 authentic pulse samples and 16,259 negative samples caused by RFI/noise. However, it only provides parameter files rather than detailed observational data, limiting the available information.

Although the LOTAAS1 dataset (Sanidas et al. 2019) comprises 66 pulsars and 4987 non-pulsar candidates discovered during the project, it is currently not publicly available.

The SPARKESX datasets (Single-dish PARKES data sets for finding the unEXpected) (Yong et al. 2022) intend to identify pulsars, FRBs, and other signals while supporting the development of new search algorithms. It contains three mock surveys from the Parkes ”Murriyang” radio telescope, providing vast sample datasets, including authentic and simulated high-time resolution observations. However, the positive samples in the datasets are simulated pulse signals of different types rather than genuine observed FRBs. Therefore, it may be less helpful in conducting specific FRB searches.

The Blinkverse (Xu et al. 2023) database² collects fast radio bursts released by various observatories, including FAST, CHIME, GBT, and Arecibo, and provides thousands of previously unavailable dynamic spectra from FAST. This comprehensive database features detailed pulse attributes, dynamic spectrograms, and source information, but does not provide detailed observational data.

Currently, based on the substantial volume of observational data, researchers have begun integrating machine learning algorithms into FRB exploration. The high-quality machine learning models perform real-time, efficient searches. For instance, employing a convolutional neural network to FRB121102 integrates neural

² <https://blinkverse.alkaidos.cn/>

network detection and dispersion removal verification, resulting in better sensitivity, lower false detection rate, and faster processing speed than conventional algorithms. The convolutional neural network detected new pulses in data obtained on August 26, 2017, where 21 bursts had been previously identified (Zhang et al. 2018). Moreover, Bo Han Chen and colleagues presented a technique for detecting repeating FRBs based on Uniform Manifold Approximation and Projection (UMAP). They discovered that unsupervised UMAP classification had a 95% completeness rate for identifying repeating FRBs and identified 188 potential sources of FRB repeaters from 474 non-repeating sources (Chen et al. 2022). Thus, creating datasets for advancing research in machine learning algorithms is paramount.

In response to the issues described above, we will offer an open-access dataset FAST-FREX of FRB signals obtained from observations made by FAST. The dataset contains authentic FRB signal samples instead of simulated ones. Since the FRB signal samples originate entirely from the observation data from FAST, they can more precisely represent real-world scenarios.

3. DATASET

3.1. Data Collection

We created our dataset by using the observational data of FRB20121102(Li et al. 2021), FRB20180301(Laha et al. 2022) and FRB20201124(Zhang et al. 2022; Niu et al. 2022b). The FAST continuous monitoring of FRB20121102 commenced in August 2019, leading to the detection of 1,652 independent burst events between August 29th and October 29th within 59.5 hours. Meanwhile, FAST observed FRB20180301 on 2021 March 4th, 9th, and 19th and detected five bright radio bursts. More than 800 bursts were detected from FRB20201124 by FAST between 2021 September 25th and 28th. The dataset comprises 470 signals from FRB20121102, 5 signals from FRB20180301, and 125 signals from FRB20201124.

These observations gathered data using 4096 frequency channels over 1.05 GHz to 1.45 GHz, with 0.122 MHz frequency resolution. These channels recorded four polarization signals. FRB20121102 has a 98.304 μ s sampling rate, while others have a 49.152 μ s sampling rate. The raw observation data was stored in FITS³ format and divided into blocks of 128 or 256 time samples. The samples were recorded in consecutive lines (or sub-integrations) in a file with 1024 samples per sub-integration.

³ <https://fits.gsfc.nasa.gov/>

Our objective is to develop and compare algorithms that can identify FRB events. Therefore, we selected 600 bursts to create positive data samples and ensured that each positive sample contained only one FRB event. In order to preserve the integrity of FRB events, we set the cropping duration of each positive sample file to about 6 seconds. We also ensure that the events appear randomly within the observation time covered by the file rather than setting a fixed Time of Arrival (ToA). This approach simulates FRB detection more realistically and enhances the dataset’s diversity, which is beneficial for algorithm research. We reduced the data size by averaging the first two polarization signals while maintaining the signal’s integrity and mitigating the noise’s effect to some extent. After eliminating the records of authentic events, we extracted 1000 negative samples of RFI and noise with the same duration as the positive samples.

3.2. Dataset Features

The dataset comprises two file types: sample files and parameter files. The sample files, stored in FITS format, contain pre-cropped observation data. Among them are 600 positive sample files containing FRB signals and 1000 negative sample files containing RFI and noise. The FRB20121102 sample file has a time sampling point of 60 * 1024, while other sources’ sample files have 120 * 1024. Moreover, the sample file’s number of polarization channels is reduced to one, which differs from the original data. The size of each file is approximately 244 MB or 488 MB, depending on its time sampling rate. Meanwhile, parameter files are stored in CSV format to record various FRB parameters for each positive sample file (see Table 1).

Table 1. Parameters of Dataset

Name	Abbr	Unit
Modified Julian Day	MJD	-
Time of Arrival	ToA	s
Dispersion Measure	DM	pc cm^{-3}

Each positive sample file contains only one FRB signal and its parameters are recorded in a corresponding parameter file specific to a fixed FRB source. In contrast, negative sample files do not have a corresponding parameter file.

MJD is an astronomical unit of recording time. We use it to record the surface observation time when the FRB signal arrives. While *ToA* counts the seconds in the data file before the FRB signal arrived. *DM* is the abbreviation for dispersion measure. Moreover, utilizing

Equation 1, it is plausible to estimate the time lag due to the dispersion phenomenon. D is the dispersion constant with a value of $4.15 \times 10^3 \text{ MHz}^2 \cdot \text{pc}^{-1} \cdot \text{cm}^3 \cdot \text{s}$. Due to the dispersion phenomenon, the high-frequency component v_2 reaches the receiver earlier than the low-frequency component v_1 . The receiver records the signals transmitted by both frequencies and their time difference.

$$t_2 - t_1 = D \times \left(\frac{1}{v_1^2} - \frac{1}{v_2^2} \right) \times DM \quad (1)$$

3.2.1. Authentic Single Pulses

From bursts of multiple FRB sources, we carefully chose 600 signals, which have a wide-spread distribution across four dimensions: (1) Full Width at Half Maximum ($FWHM$), (2) *bandwidth*, (3) peak flux density (S_{peak}), and (4) fluence (F), to form the positive samples. This approach ensures the diversity of FRB signals in our dataset. Figure 1 depicts the distribution of these four parameters.

The $FWHM$ is a parameter commonly used to describe the width of the burst profile. It is given by the distance between points on the spectral curve at which the intensity reaches half its peak. The burst is distributed over a frequency interval, and the range of this frequency interval is called *bandwidth*. The spectral flux density is a quantity that indicates the observed strength of an astronomical source. It is a measure of the strength of a radio signal received from a discrete source, which is measured in watts per square meter per hertz ($\text{W m}^{-2} \text{ Hz}^{-1}$). Peak flux density S_{peak} is the maximum flux intensity of the pulse profile. The unit of flux density is the jansky (Jy), and 1 Jy equals $10^{-26} \text{ W m}^{-2} \text{ Hz}^{-1}$. The fluence F of a burst is computed by integrating the burst profile concerning time and *bandwidth*, which is used to describe the total energy of the burst. The unit of F is Jy ms.

The DM range of these signals is limited, lying between 411.51 and 570.0 pc cm^{-3} . Pulse widths are varied over a range of 0.34 to 78.52 ms. The minimum S_{peak} is 0.00169 Jy, while the maximum is 0.84239 Jy. Moreover, the *bandwidth* is between 16 and 500 MHz, and the F is between 0.0016 and 4.5616 Jy ms. These data are collected from the cited articles.

In Figure 2, we present the frequency-time domain representation of FRB signals, varying pulse width of positive samples. Pulse width indicates the duration of the FRB signals on the time axis. Figure 3 displays the frequency-time domain of FRB signals, with varying signal flux densities of positive samples. This visualization illustrates that signals with higher flux density are more prominently observed than the background noise.

3.2.2. Radio Frequency Interference

Based on FAST observations, we can categorize RFI in FAST data into three types: (1) narrow-band RFI, (2) 1 MHz-wide RFI, and (3) fixed frequency RFI with broader bandwidth (Jiang et al. 2020). Narrow-band RFI can have various origins, such as interference from electronic devices or local effects of the telescope. The 1 MHz wide RFI is caused by the standing wave, which looks like a regular sinusoidal wave or the single bump in FAST spectra. The fixed frequency RFI is due to satellite or civil aviation from the sky. Several examples of negative samples are shown in Figure 4, where the bright yellow patches are predominantly fixed frequency RFI (type 3). In contrast, the first two types of RFI are challenging to discern visually. We selected RFI and noise randomly from the original observation files instead of simulated RFI injection. Similar to the positive samples, these negative samples possess diversity and represent real-world scenarios, as depicted in Figure 4.

4. METHODS

4.1. RaSPDAM

The RaSPDAM algorithm aims to identify FRB/PSR(PulSaR) signals using a computer vision-based approach, demonstrating significant enhancements in both efficiency and accuracy.

In conventional approaches, the initial step of searching for FRBs involves de-dispersion, a process that requires significant time and computational resources (CPU/GPU cores) to perform the Fast Fourier Transform (FFT) operation. As a result, the process of searching for FRBs has become computationally intensive and time-consuming. In the context of RaSPDAM, observational data is processed as conventional images. The signal sequence is segmented and converted into an image format with dimensions of 512×512 pixels. The image serves as the input for a semantic segmentation model.

4.1.1. Signal Preprocessing & Enhancement

The initial step is to convert the original signal sequence into standard images without de-dispersion. The signal sequence is divided into smaller slices within a 2-second width sliding window and a 1-second overlap. To standardize the model input, we resized the image slices to dimensions of 512×512 .

The second step in preparing for segmentation is image enhancement. Typically, the FRB signal appears as a curve overlapped with noise in a sequence of signals. Initially, we use convolution to enhance the characteristics of the curve. In image processing, convolution transforms an image by applying a kernel to each pixel and its local neighbors across the entire image. For this case, as shown in Figure 5, we utilize multiple convo-

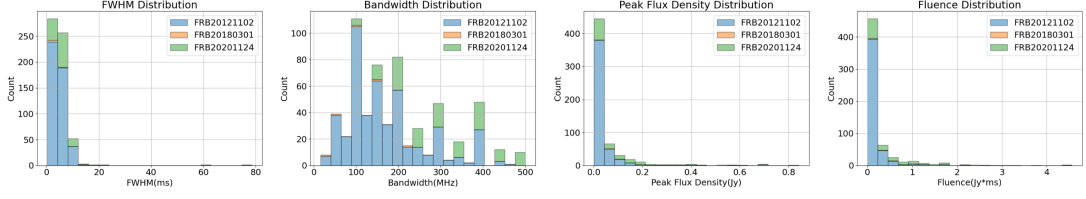


Figure 1. Distribution of feature parameters for FRBs

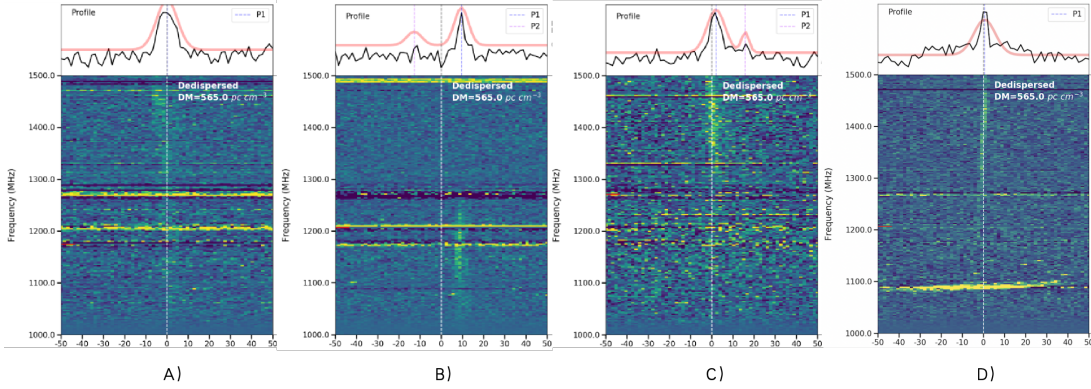


Figure 2. Examples of positive samples with different pulse widths

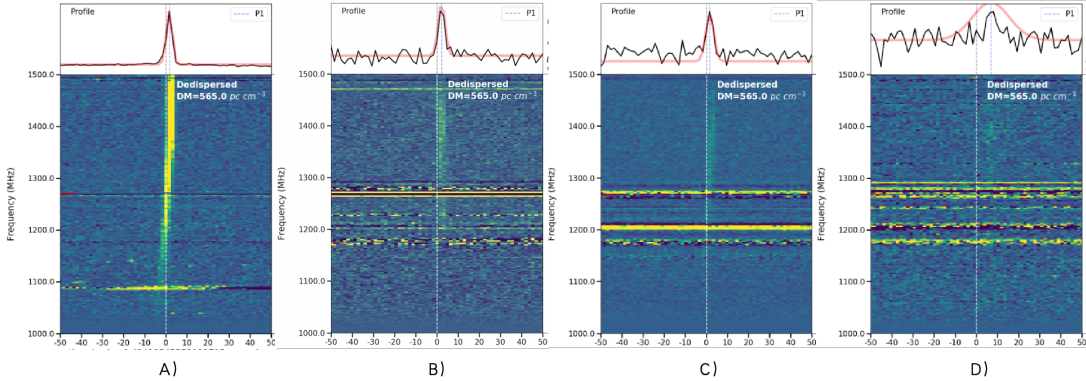


Figure 3. Examples of positive samples with different flux densities

lution kernels generated from fixed curve slopes. After convolving the image slices with multiple convolution kernels, we apply morphological dilation to further enhance the signal. Finally, to maximize the utilization of image features, the enhanced images (post-convolution and after morphological dilation) and the original image have been combined into an RGB image, which will be used as the model input. Figure 5 illustrates an example of this process.

4.1.2. Model Training

The aim of FRB detection resembles semantic segmentation, also known as pixel-based classification. It requires a method to differentiate the FRB signal component from the background, where noise might interfere with segmentation outcomes. In this case, we choose the UNet as the model implementation due to several key advantages:

1. *High-performance*: UNet is recognized for generating accurate segmentation maps, particularly when

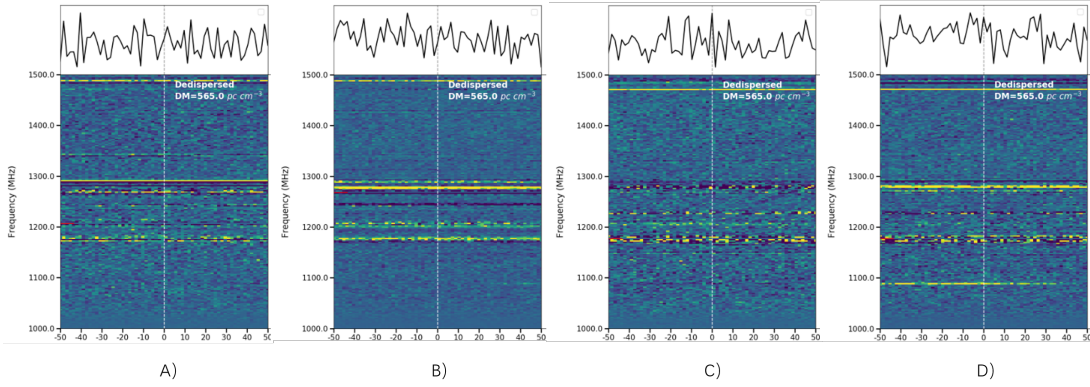


Figure 4. Examples of negative samples

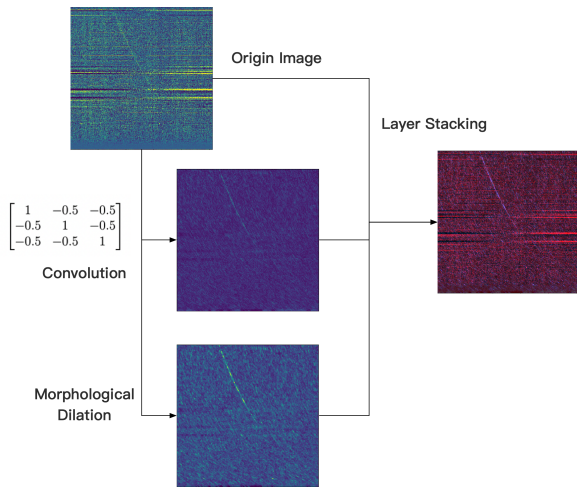


Figure 5. Signal Image Preprocessing Procedure

handling high-resolution images or datasets with numerous classes.

2. *Efficiency*: UNet incorporates high-level and low-level features from the input image depending on skip connections. It enhances the model’s efficiency in utilizing training data, improving overall performance.

Unet is a Convolutional Neural Network specialized in classification tasks, localizing specific areas by classifying individual pixels. The architecture resembles a U-shape, with the left side part known as the encoder or contracting path and the right side as the decoder or expansion path.

Training the network requires a significant amount of FRB signal images. However, there is a lack of available training data in the field of astronomy. Our proposed alternative involves generating simulated FRB signals. As previously mentioned, we enhance the signal sequence slice using convolution kernels. To generate simulated

signals, we apply a similar process by using random curve slopes and Gaussian noises. With the known slope of the FRB curve, it is possible to accurately determine its position and create mask images for training purposes.

4.1.3. Candidate Identification

The network segmentation process produces segmentation maps for the purpose of identifying potential candidates for FRB signals. However, it may still contain noise. In response to this issue, we have implemented multiple procedures for candidate identification.

Figure 6 shows that we utilize the “regionprops” function for the analysis of connected areas. Each identified candidate is quantified as x , while the area of the region box and the filled area are represented as $area_bbox$ and $area_filled$. Then, we use thresholds t_a . If t_a is smaller than the ratio of $area_filled$ to $area_bbox$, it is flagged as noise, as indicated in Equation 2.

$$F(x) = \begin{cases} \frac{x.area_filled}{x.area_bbox} < t_a \\ \frac{x.x_2 - x.x_1}{window_width} > t_b \\ \frac{x.y_2 - x.y_1}{window_height} > t_c \end{cases} \quad (2)$$

Additionally, we calculate the candidate’s projection on both the x-axis and y-axis. Candidates exceeding both x-axis and y-axis projections above thresholds that denoted as t_b and t_c , as potential FRB signals.

4.2. Conventional Methods

In addition to the machine learning algorithm RaSP-DAM described above, we established baseline models using conventional single-pulse search software, including PRESTO and Heimdall. The search process for astronomical signals contains RFI removal, de-dispersion, and matched filtering and generates single pulse candidates. Interstellar media can interfere with the arrival time of high-frequency and low-frequency electromagnetic waves

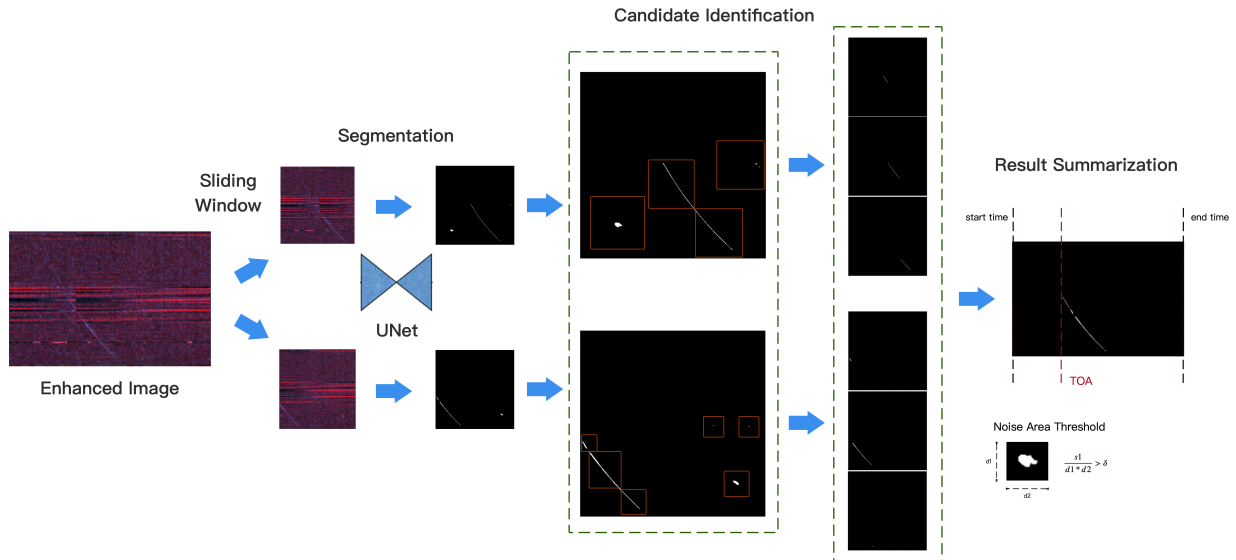


Figure 6. Candidate Identification

to radio telescopes. This phenomenon results in energy dispersion of astronomical signals, broadening of pulse profiles, decreased signal-to-noise ratio, or even disappearance of the pulse signal. To overcome these effects, PRESTO and Heimdall process the original signal using the principle of non-coherent de-dispersion before conducting single-pulse searching. This step compensates for different frequency-time delays, eliminating the effects of frequency-related delays and improving the signal-to-noise ratio.

4.2.1. PRESTO

PRESTO has many options to optimize the FRB search tasks. We choose a simple set of parameters as representative PRESTO output. The search pipeline includes RFI removal, de-dispersion, and single-pulse search. We identified and marked narrowband and short-duration broadband interference in the data as RFIs, recording it in ".mask" files to facilitate removal. Due to the range of dispersion in the dataset, we set the DM grid range from 350 pc cm^{-3} to 650 pc cm^{-3} and the DM grid density at 1. The de-dispersion task with the above DM grid was applied to the dataset, leading to a set of de-dispersed time series. A single-pulse search was conducted for each DM value to detect pulses surpassing a Signal-to-Noise Ratio (SNR) threshold of 3.0, which were then cataloged in a candidate list.

4.2.2. Heimdall

Heimdall is a GPU-accelerated transient detection pipeline. It computes the search step based on smearing calculations for each DM value to balance computational requirements more evenly across the entire DM range, resulting in better dispersion removal at higher disper-

sion measures. Heimdall pipeline includes de-dispersion, baseline removal, normalization, matched filtering, re-normalization, and SNR threshold filtering. In the matched filtering step, a DM range of 350 pc cm^{-3} - 650 pc cm^{-3} was chosen as same as PRESTO.

5. BENCHMARKS AND RESULTS

5.1. Baseline Scoring Metrics

We aim to improve the efficiency and accuracy of identifying positive samples containing FRB signals. Consequently, our approach yields metrics, including recall and precision rates. The True Positives (TPs) and True Negatives (TNs) mean the correctly predicted positive candidates and negative samples. Meanwhile, False Positives (FPs) and False Negatives (FNs) reflect the erroneously predicted positive candidates and negative samples. We define that detecting FRB signal candidates in positive samples with a ToA error $\leq 0.2\text{s}$ and a DM error $\leq 50 \text{ pc cm}^{-3}$ are correctly predicted TPs. Candidates in positive samples that do not meet the specified error thresholds and candidates found in negative samples are FPs. Consequently, the number of FPs may exceed the number of sample files, as each sample file could yield multiple candidates. If no FRB signal candidates appear in negative samples, they are correctly predicted as negative samples (TNs). If no candidates are found in positive samples, it is treated as FNs.

For the RaSPDAM algorithm, considering its image identification method, the DM value cannot be measured. Therefore, the determination of TP relies solely on ToA . Additionally, it cannot precisely calculate the ToA . Hence, if the ToA of a candidate falls within the

signal’s entire period or has an error $\leq 0.2s$, it should be classified as a TP.

Recall measures the number of correctly predicted positive samples and the FRB search algorithm’s coverage. This measure is critical because it signifies our capacity to identify more FRB signals and indicates the level of completeness of the search. In this paper, we use TP/P to calculate the recall rate.

Precision measures correctly predicted positive samples among all predicted samples. This metric directly affects the judgment of the FRB search’s results, and low precision will result in high labor costs for secondary screening. We use TP/(TP+FP) to calculate the precision rate.

F1 score is a metric for evaluating classification problems. It is the harmonic mean of precision and recall.

$$F1 = 2\left(\frac{1}{Recall} + \frac{1}{Precision}\right)^{-1} \quad (3)$$

5.2. Results

We run our baseline tasks on a server with 2 Intel(R) Xeon(R) Platinum 8358 CPUs (32 cores 2.6GHz), 1TB memory, and 8 NVIDIA A40 GPUs. PRESTO, Heimdall, and RaSPDAM were deployed to process the dataset with the parameters mentioned above, and the results are presented in Table 2. To process a single sample file of FRB20121102, PRESTO took an average of 141.96 seconds on 1 CPU, Heimdall took an average of 6.98 seconds on 1 GPU, while RaSPDAM only took an average of 3.37 seconds on 1 GPU.

As mentioned in previous sections, different from conventional softwares, RaSPDAM directly converts signal sequences into images rather than spending more computational resources on performing dedispersion. For RaSPDAM, the FITS file only needs to be scanned once, reducing time complexity. Furthermore, in the implementation, the image transformation and model segmentation steps have been accelerated by GPU. Thus, RaSPDAM shows significant speedup in most cases.

The results indicate that PRESTO and Heimdall have a higher recall rate than the machine learning algorithm RaSPDAM on the total dataset. However, the accuracy of RaSPDAM is very high, whereas both PRESTO and Heimdall are unsatisfactory. Due to the misidentification of RFI as genuine signals, PRESTO and Heimdall calculate a significantly larger number of detected signals than true FRBs. As a result, the absence of human intervention makes it difficult for the two conventional softwares to screen out true FRB signals effectively.

None of the three search pipelines can identify all of the FRB signals according to the final testing results. For conventional software, refining the *DM* grid and reducing

the SNR threshold may improve the recall rate but may lead to even lower precision. For FRB20121102 samples in our dataset, we reduced PRESTO’s *DM* grid to 0.05 pc cm^{-3} but observed nearly no recall rate changes while the precision rate increases. Nevertheless, raising the SNR threshold in PRESTO to 5.0 decreased the recall rate from 0.7745 to 0.6957 and increased the precision rate from $2.1469E-05$ to 0.0110. In conclusion, to tackle the issue observed in PRESTO, it is essential to advance RFI removal methods, which may overlook specific FRB signals during RFI removal. Regarding Heimdall, a more in-depth exploration of the code may be necessary for adjustments due to its limited adjustable parameters. Given that the RaSPDAM algorithm is trained based on simulated signals, a strategy for improvement would be fine-tuning the model using authentic data.

Moreover, as depicted in Figure 7, the performance of the methods varies across different FRB sources due to the inherent differences in FRB attributes among sources. Subsequently, we intend to expand our dataset by incorporating additional sources to enhance its comprehensiveness.

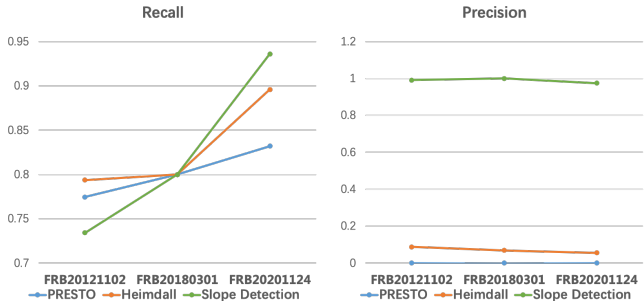


Figure 7. Methods Evaluation Metrics on Different FRB Sources

6. APPLICATION

6.1. Distributed Computing Architecture

To address the challenge of processing petabyte-scale data generated by FAST, we adopted a distributed computing architecture based on Kubernetes⁴ and Airflow⁵. This architecture significantly extends our data processing capabilities, enabling the efficient handling of massive datasets.

1. *Data Processing Pipeline*: We used Airflow’s Directed Acyclic Graph (DAG) to construct the data

⁴ <https://kubernetes.io/>

⁵ <https://airflow.apache.org/>

Table 2. Methods Running Results: Confusion Matrix and Evaluation Metrics

Software	Confusion Matrix							Evaluation Metrics		
	N	P	N+P	TN	TP	FN	FP	Recall	Precision	F1 Score
PRESTO	1000	600	1600	3	472	0	26963700	0.7867	1.7505E-05	3.5009E-05
Heimdall	1000	600	1600	218	489	36	5854	0.8150	0.0771	0.1409
RaSPDAM	1000	600	1600	989	466	128	6	0.7767	0.9873	0.8694

processing pipeline. This pipeline includes not only the core algorithm processing but also pre- and post-processing steps such as data cleaning and data organization. It ensures the completeness and continuity of the data processing workflow.

- 2) *Dynamic Task Partitioning*: We employed Airflow’s Dynamic Task Mapping feature, which allows for dynamically mapping large data tasks to different processing nodes. Based on the characteristics of the tasks and available resources, tasks are assigned to the most optimal computing nodes. This approach maximizes resource utilization and optimizes task execution efficiency.

6.2. Discoveries of RaSPDAM

The RaSPDAM algorithm has been successfully implemented in FRB and pulsar studies. Since its deployment last year, our team has leveraged this algorithm to identify 2 FRBs (FRB20211103A and FRB20230104) and 80 pulsars. Among these pulsar detections, 13 are previously undiscovered pulsars, highlighting the algorithm’s efficacy in uncovering new celestial objects. Table 3 presents a compilation of these pulsars.

7. DISCUSSION

We provide the FAST-FREX dataset, offer a new machine learning algorithm, RaSPDAM, and use the experiment results of the conventional single-pulse search software PRESTO and Heimdall, along with RaSPDAM as the baseline. The results demonstrate excellent room for progress regarding recall, precision, and performance. Designing and developing new search processes based on machine learning algorithms is a solution. Researchers can also explore machine learning algorithms combined with PRESTO and Heimdall, such as FETCH (Connor & van Leeuwen 2018), which can reduce the costs of manual screening. The following are some limitations that should be considered when developing machine learning algorithms using the FAST-FREX dataset:

- 1) a single sample file in our dataset contains either no or one FRB signal. However, most observation files from radio telescopes are significantly longer, containing multiple FRB signals; in some cases, some of the signals may be truncated. When applying newly designed

machine learning algorithms to these data, data preprocessing (split or merge) is essential to prevent missing FRB signals at the edges of observation files.

- 2) Our dataset currently only includes 600 signals from three FRB sources and RFI/noise observed from the specific observations. However, due to variations in observational conditions and intrinsic properties of FRBs, unexpected patterns possibly exist in unknown candidates, which causes models trained on this dataset to fail to recognize other signals. The Blinkverse (Xu et al. 2023) database accumulated an impressive catalog of 8,007 FRB bursts from 813 FRB sources (data up to May 27, 2024), including the bursts our dataset collected. In future work, we aim to extend the dataset with more FRBs, guided by the comprehensive records within Blinkverse, to enhance the comprehensiveness of our dataset.

Furthermore, RaSPDAM can only provide the ToA as a result, while other algorithms provide both ToA and DM , which may cause inconvenience in candidate verification. For future work, we will continue to enhance the capabilities of RaSPDAM to provide more comprehensive features. In addition, in previous model training, we only used simulated FRB signals, which may differ from real signals. We will try to fine-tune the model with real signals in the future, which may further improve the recall rate.

8. CONCLUSION

This paper presents the FAST-FREX dataset for FRB search based on FAST observation data. Furthermore, we developed a new machine learning algorithm, RaSPDAM, with higher precision, better performance, and a considerable recall rate. Also, we present the benchmark results of conventional FRB search pipelines, PRESTO and Heimdall, which can serve as reference points for future algorithm research.

The dataset aims to support the development of machine learning algorithms for searching FRB signals, such as the method proposed in (Zhang et al. 2024). To ensure comprehensive coverage of the entire parameter space for FRB signals, we plan to collect more FRB signals from observation data acquired by FAST in the future. Moreover, to harness the potential of Artificial Intelligence (AI) for improving the efficiency of pulsar searches and

Table 3. Pulsars found by RaSPDAM

No.	Pulsar	New Discovery	No.	Pulsar	New Discovery
1	19C107_J0528+04		41	PSR J0652+0142	
2	19C147_J0104+6127	Yes	42	PSR J0741+17	
3	19C148_J0145+6020	Yes	43	PSR J1628+4406	
4	19C149_J2114+2630	Yes	44	PSR J1822+2617	
5	19C150_J0114+6149	Yes	45	PSR J1829+25	
6	19C151_J0000+6250	Yes	46	PSR J1908+2351	
7	19C152_J0231+6254	Yes	47	PSR J1911+37	
8	19C155_J1958+2332	Yes	48	PSR J1912+2525	
9	19C156_J1924+2354	Yes	49	PSR J1919+2621	
10	19C158_J1735+3613	Yes	50	PSR J1929+3817	
11	19C159_J2131+3642	Yes	51	PSR J1938+2659	
12	19C160_J1726+3707	Yes	52	PSR J1939+2449	
13	19C171_J0009+5923	Yes	53	PSR J1939+2609	
14	19C173_J0642+0238	Yes	54	PSR J1941+2525	
15	C10_J0209+2621		55	PSR J1946+2535	
16	PSR J0033+61		56	PSR J1946+2611	
17	PSR J0058+6125		57	PSR J1946+35	
18	PSR J0116+57		58	PSR J1948+2333	
19	PSR J0125+62		59	PSR J1948+2551	
20	PSR J0139+5814		60	PSR J1954+2529	
21	PSR J0141+6009		61	PSR J1956+35	
22	PSR J0147+5922		62	PSR J1959+3620	
23	PSR J0147+5922		63	PSR J2005+3547	
24	PSR J0157+6212		64	PSR J2005+3552	
25	PSR J0215+6218		65	PSR J2008+2513	
26	PSR J0243+6027		66	PSR J2008+3758	
27	PSR J0248+6021		67	PSR J2016+38	
28	PSR J0343+06		68	PSR J2019+3718g	
29	PSR J0358+4155		69	PSR J2019+3810	
30	PSR J0413+58		70	PSR J2021+3651	
31	PSR J0435+2749		71	PSR J2026+3656g	
32	PSR J0447+04		72	PSR J2027+37	
33	PSR J0458+0505		73	PSR J2030+3641	
34	PSR J0459+0210		74	PSR J2037+3621	
35	PSR J0459+0210		75	PSR J2045+3633	
36	PSR J0601+0527		76	PSR J2055+3630	
37	PSR J0608+1635		77	PSR J2102+38	
38	PSR J0624+0424		78	PSR J2116+3701	
39	PSR J0625+17		79	PSR J2156+2618	
40	PSR J0627+16				

enabling the exploration of pulsars in closed binary systems, we envision the development of a dataset designed for pulsar search tasks.

The dataset is publicly and freely available to the scientific community (<https://www.scidb.cn/en/s/VfaYNr>). Based on FAST-FREX, a FRB search algorithm challenge will be held to accelerate the research of machine learning algorithms in this field. Meanwhile, we hope that the FAST-FREX dataset serves not only as a facilitator for AI applications in FRB search but also as a catalyst for the advancement of AI for Science.

APPENDIX

A. FAST-FREX DATASHEET

In this section, we will comply with the guidelines presented in "Datasheets for Datasets"⁶ to provide detailed documentation of the FAST dataset for Fast Radio bursts EXploration (FAST-FREX). Therefore, we will address specific sections that include queries related to the dataset's motivation, composition, collection process, pre-processing/cleaning/labeling, options for usage, distribution, and maintenance. We will distinguish each section's primary and subsequent questions using bold and italic fonts.

A.1. Motivation

- *For what purpose was the dataset created?—Was there a specific task in mind? Was there a specific gap that needed to be filled?*

The FAST-FREX dataset aims to assist researchers in developing advanced machine learning algorithms for searching Fast Radio Burst (FRB) signals. We hope that the FAST-FREX dataset serves not only as a facilitator for Artificial Intelligence (AI) applications in FRB search but also as a catalyst for advancing AI for Science.

- *Who created the dataset (e.g., which team, research group) and on behalf of which entity (e.g., company, institution, organization)?—*

The Research Center for Astronomical Computing of Zhejiang Laboratory created the dataset. The Zhejiang Laboratory and National Astronomical Observatories, Chinese Academy of Sciences (NAOC) are on behalf of the dataset.

- *Who funded the creation of the dataset?—If there is an associated grant, please provide the name of the grantor and the grant name and number.*

This work is partially supported by the National Natural Science Foundation of China (NSFC) (11988101). Di Li is a New Cornerstone investigator. This work is also supported by Key R&D Program of Zhejiang (2024SSYS0012). This work made use of the observation data from FAST (Five-hundred-meter Aperture Spherical radio Telescope). FAST is a Chinese national mega-science facility, operated by National Astronomical Observatories, Chinese Academy of Sciences.

Astronomical Big Data Service Platform Project of the Zhejiang Laboratory funded this dataset. And this work is partially supported by the National Natural Science Foundation of China (NSFC) (11988101). This work is also supported by Key R&D Program of Zhejiang (2024SSYS0012).

- *Any other comments?—*
No.

A.2. Composition

- *What do the instances that comprise the dataset represent (e.g., documents, photos, people, countries)?—Are there multiple types of instances (e.g., movies, users, and ratings; people and interactions between them; nodes and edges)?*

The FAST-FREX comprises two file types: sample file and parameter file. The sample files, stored in FITS format, contain pre-cropped observation data. The parameter files, stored in CSV format, record various parameters of FRBs in positive samples.

- *How many instances are there in total (of each type, if appropriate)?—*

The dataset contains a total of 1600 instances that are divided into 600 positive sample files containing FRB signals and 1000 negative sample files containing Radio Frequency Interference (RFI) and noise.

- *Does the dataset contain all possible instances or is it a sample (not necessarily random) of instances from a larger set? —If the dataset is a sample, then what is the larger set? Is the sample representative of the larger set (e.g., geographic coverage)? If so, please describe how this representativeness was validated/verified. If it is not representative of the larger set, please describe why not (e.g., to cover a more diverse range of instances, because instances were withheld or unavailable).*

We carefully chose 600 authentic FRB signals from individual bursts of FRB20121102, FRB20180301, and

⁶ <https://arxiv.org/abs/1803.09010>

FRB20201124 as positive examples. To guarantee the diversity of FRB signals in our dataset, we make sure the positive samples have a wide-spread distribution across four dimensions: (1) Full Width at Half Maximum ($FWHM$), (2) *bandwidth*, (3) peak flux density (S_{peak}), and (4) fluence (F). We intend to extend the dataset with more FRB signals to cover the entire parameter space for FRB signals comprehensively.

- *What data does each instance consist of?—“Raw” data (e.g., unprocessed text or images) or features? In either case, please provide a description.*

Each instance includes observation data in FITS ⁷ format with 60 * 1024 time sampling points, a 98.304 μm or 49.152 μs sampling rate, and a single polarization channel. The size of each sample file is approximately 244 MB or 488MB, depending on its sampling rate. Parameter files are stored in CSV format to record various FRB parameters of positive sample files.

- *Is there a label or target associated with each instance?—If so, please provide a description.*

Yes. Each positive sample file only contains one FRB signal and has a corresponding parameter file. The parameter description file includes the FRB signal’s *ToA* (Time of Arrival), *DM*, and *MJD*. It should be noted that *MJD*, in this context, refers to surface observation time rather than arrival time at the solar system barycenter after correcting the frequency to 1.5GHz. Negative sample files do not have a corresponding parameter file.

- *Is any information missing from individual instances?—If so, please provide a description, explaining why this information is missing (e.g., because it was unavailable). This does not include intentionally removed information, but might include, e.g., redacted text.*

We reduced the sample data size by averaging the first two polarization signals while maintaining the signal’s integrity and mitigating the noise’s effect to some extent. The parameter file for the positive samples only includes parameters related to FRB search, such as *ToA* and *DM*. Other information, including *FWHM*, *bandwidth*, S_{peak} , and F , are not provided because they are not helpful for FRB search. Instead, these parameters are primarily used for analyzing the detected FRB signals.

- *Are relationships between individual instances made explicit (e.g., users’ movie ratings, social network links)?—If so, please describe how these relationships are made explicit.*

Yes. The FRB signal in each instance is independent and chosen from the sources FRB20121102, FRB20180301, and FRB20201124.

- *Are there recommended data splits (e.g., training, development/validation, testing)?—If so, please provide a description of these splits, explaining the rationale behind them.*

No.

- *Are there any errors, sources of noise, or redundancies in the dataset?—If so, please provide a description.*

Both positive and negative sample files contain noise and RFI because they are inevitable during the Five-hundred-meter Aperture Spherical radio Telescope (FAST) observations.

- *Is the dataset self-contained, or does it link to or otherwise rely on external resources (e.g., websites, tweets, other datasets)?—If it links to or relies on external resources, a) are there guarantees that they will exist, and remain constant, over time; b) are there official archival versions of the complete dataset (i.e., including the external resources as they existed at the time the dataset was created); c) are there any restrictions (e.g., licenses, fees) associated with any of the external resources that might apply to a dataset consumer? Please provide descriptions of all external resources and any restrictions associated with them, as well as links or other access points, as appropriate.*

Our dataset is entirely self-contained and comprises samples collected from publicly available FAST observation data ⁸.

- *Does the dataset contain data that might be considered confidential (e.g., data that is protected by legal privilege or by doctor-patient confidentiality, data that includes the content of individuals’ non-public communications)?—If so, please provide a description.*

No.

- *Does the dataset contain data that, if viewed directly, might be offensive, insulting, threatening, or might otherwise cause anxiety?—If so, please describe why.*

No.

A.3. Collection Process

- *How was the data associated with each instance acquired?—Was the data directly observable (e.g., raw text, movie ratings), reported by subjects (e.g., survey responses), or indirectly inferred/derived from other data (e.g., part-of-speech tags, model-based guesses for age or language)?*

⁷ <https://fits.gsfc.nasa.gov/>

⁸ <https://fast.bao.ac.cn/>

If the data was reported by subjects or indirectly inferred/derived from other data, was the data validated/verified? If so, please describe how.

We build the dataset using observational data from reports on FRB20121102⁹, FRB20180301¹⁰ and FRB20201124¹¹, which contains detailed information about individual bursts observed by FAST.

- *What mechanisms or procedures were used to collect the data (e.g., hardware apparatuses or sensors, manual human curation, software programs, software APIs)?—How were these mechanisms or procedures validated?*

The raw observation data were collected from three FRB sources. The FAST continuous monitoring of FRB121102 began in August 2019. During 59.5 hours, 1,652 independent burst events were detected from August 29th to October 29th. Meanwhile, FAST observed FRB20180301 on 2021 March 4th, 9th, and 19th and detected five bright radio bursts. 881 bursts detected from FRB20201124 by FAST between 2021 September 25th and 28th. The data was gathered using 4096 frequency channels over 1.05 GHz to 1.45 GHz, with 0.122 MHz frequency resolution. FRB20121102 has a 98.304 μ s sampling rate, while others have a 49.152 μ s sampling rate. These channels recorded four polarization signals.

To preserve the integrity of FRB signals, we set the cropping duration of each positive sample file to about 6 seconds. We reduced the data size by averaging the first two polarization signals while maintaining complete signal recordings and mitigating the effect of noise to some extent. We carefully chose 600 bursts to create positive samples. After eliminating the observation data of FRB signals, we extracted 1000 negative samples of RFI and noise with the same data length as the positive samples.

- *If the dataset is a sample from a larger set, what was the sampling strategy (e.g., deterministic, probabilistic with specific sampling probabilities)?—*

This dataset is a subset of bursts from three FRB sources. Positive samples have been manually chosen and guaranteed to exhibit changes in $FWHM$, $bandwidth$, S_{peak} , and F four dimensions. Figure 1 in the paper depicts the probability distribution of these four parameters.

- *Who was involved in the data collection process (e.g., students, crowdworkers, contractors) and how were they compensated (e.g., how much were crowdworkers paid)?—*

The official staff of the Zhejiang Laboratory and NAOC collected the dataset.

- *Over what timeframe was the data collected?—Does this timeframe match the creation timeframe of the data associated with the instances (e.g., recent crawl of old news articles)? If not, please describe the time-frame in which the data associated with the instances was created.*

The raw observation data for FRB121102 was generated from August 29th to October 29th, 2019, within 59.5 hours. FRB20180301 was observed on 2021 March 4th, 9th, and 19th, and FRB20201124 was between 2021 September 25th and 28th. However, the dataset creation process was completed within a relatively short period.

- *Were any ethical review processes conducted (e.g., by an institutional review board)?—If so, please provide a description of these review processes, including the outcomes, as well as a link or other access point to any supporting documentation.*

No.

A.4. Preprocessing/Cleaning/Labeling

- *Was any preprocessing/cleaning/labeling of the data done (e.g., discretization or bucketing, tokenization, part-of-speech tagging, SIFT feature extraction, removal of instances, processing of missing values)?—If so, please provide a description. If not, you may skip the remaining questions in this section.*

To maintain the integrity of FRB signals, the cropping duration of each positive sample file was set to 6 seconds. We also ensure that the events appear randomly within the observation time covered by the file rather than setting a fixed ToA . This approach simulates FRB detection more realistically and enhances the dataset’s diversity, which is beneficial for algorithm research. We reduced the data size by averaging the first two polarization signals while maintaining the signal’s integrity and mitigating the noise’s effect to some extent. Each sample file consists of 60 * 1024 or 120 * 1024 time sampling points, and the number of polarization channels is reduced to one, which differs from the original data. The size of each file is approximately 244 MB or 488MB, depending on its sampling rate.

- *Was the “raw” data saved in addition to the preprocessed/cleaned/labeled data (e.g., to support unanticipated future uses)?—If so, please provide a link or other access point to the “raw” data.*

No. Due to the large amount of raw data, it is not convenient to store.

- *Is the software that was used to preprocess/clean/label the data available?—If so, please provide a link or other access point.*

⁹ <https://www.nature.com/articles/s41586-021-03878-5>

¹⁰ <https://iopscience.iop.org/article/10.3847/1538-4357/ac63a8>

¹¹ <http://groups.bao.ac.cn/ism/CRAFTS/FRB20201124A/>

No, but we have explained the dataset creation approach in the preceding sections.

- *Any other comments?*—
No.

A.5. Uses

- *Has the dataset been used for any tasks already?—If so, please provide a description.*

We have performed our experiments using conventional single-pulse search softwares, PRESTO and Heimdall, and a new machine learning algorithm Radio Single-Pulse Detection Algorithm Based on Visual Morphological Features (RaSPDAM), as outlined in Section 5 of this paper.

- *Is there a repository that links to any or all papers or systems that use the dataset?—If so, please provide a link or other access point.*

No.

- *What (other) tasks could the dataset be used for?—*

The dataset can be used to train and test machine learning algorithms for FRB search.

- *Is there anything about the composition of the dataset or the way it was collected and preprocessed/cleaned/labeled that might impact future uses?—For example, is there anything that a dataset consumer might need to know to avoid uses that could result in unfair treatment of individuals or groups (e.g., stereotyping, quality of service issues) or other risks or harms (e.g., legal risks, financial harms)? If so, please provide a description. Is there anything a dataset consumer could do to mitigate these risks or harms?*

No.

- *Are there tasks for which the dataset should not be used?—If so, please provide a description.*

No.

- *Any other comments?*—
No.

A.6. Distribution

- *Will the dataset be distributed to third parties outside of the entity (e.g., company, institution, organization) on behalf of which the dataset was created?—If so, please provide a description.*

Yes, the dataset is openly distributed to third parties outside the entity on behalf of which the dataset was created. It is an open-source dataset for anyone to access, use, and share for noncommercial purposes.

- *How will the dataset will be distributed (e.g., tarball on website, API, GitHub)?—Does the dataset have a digital object identifier (DOI)?*

The URL to access the dataset is <https://www.scidb.cn/en/s/VfaYNr>.

- *When will the dataset be distributed?—*

The dataset is publicly accessible.

- *Will the dataset be distributed under a copyright or other intellectual property (IP) license, and/or under applicable terms of use (ToU)?—If so, please describe this license and/or ToU, and provide a link or other access point to, or otherwise reproduce, any relevant licensing terms or ToU, as well as any fees associated with these restrictions.*

The dataset is openly shared under the CC BY-NC-ND 4.0 license.

- *Have any third parties imposed IP-based or other restrictions on the data associated with the instances?—If so, please describe these restrictions, and provide a link or other access point to, or otherwise reproduce, any relevant licensing terms, as well as any fees associated with these restrictions.*

No.

- *Do any export controls or other regulatory restrictions apply to the dataset or to individual instances?—If so, please describe these restrictions, and provide a link or other access point to, or otherwise reproduce, any supporting documentation.*

No.

- *Any other comments?*—

No

A.7. Maintenance

- *Who will be supporting/hosting/maintaining the dataset?*

The Zhejiang Laboratory will host and maintain the dataset.

- *How can the owner/curator/manager of the dataset be contacted (e.g., email address)?—*

Please reach out to Huaxi Chen (chen-huaxi@zhejianglab.com) and Xuerong Guo (guoxr@zhejianglab.com), the authors of this paper.

- *Is there an erratum?—If so, please provide a link or other access point.*

No.

- *Will the dataset be updated (e.g., to correct labeling errors, add new instances, delete instances)?—If so, please describe how often, by whom, and how updates will be*

communicated to dataset consumers (e.g., mailing list, GitHub)?

Our dataset will be periodically updated to add more samples from various FRB sources. Subsequent modifications will be reported on its public website.

- If the dataset relates to people, are there applicable limits on the retention of the data associated with the instances (e.g., were the individuals in question told that their data would be retained for a fixed period of time and then deleted)?—If so, please describe these limits and explain how they will be enforced.

No.

- Will older versions of the dataset continue to be supported/hosted/maintained?—If so, please describe how. If not, please describe how its obsolescence will be communicated to dataset consumers.

Yes, information on updates and maintenance will be regularly posted on its public website.

- If others want to extend/augment/build on/contribute to the dataset, is there a mechanism for them to do so?—If so, please provide a description. Will these contributions be validated/verified? If so, please describe how. If not, why not? Is there a process for communicating/distributing these contributions to dataset consumers? If so, please provide a description.

No.

- Any other comments?—

No

A.8. Responsibility

The authors bear all responsibility for rights violations of the FAST-FREX dataset.

B. READING AND USING THE DATASET

The sample files are stored in the standard FITS format and can be accessed through the Python library *astropy*. These files comprise two Header and Data Unit (HDU) components. Observation parameters are stored in the headers of the first and second HDU, while observation data are stored in the second HDU. The observation data contains five dimensions: 1) the first two dimensions consist of 60 * 1024 or 120* 1024 time sampling points, 2) the third dimension represents one polarization, 3) the fourth dimension includes 4096 frequency channels, and 4) the fifth dimension is currently unused.

Please note that because the sample files were generated from the raw observation files, the start *MJD* time parameters do not apply to the current sample files, particularly the *STT_IMJD*, *STT_SMJD*, and *STT_OFFS* parameters in the first header (*f[0].header* in the following code).

Please refer to the code example below for specifics.

```

1 from astropy.io import fits
2
3 with fits.open('./FRB20121102/FRB20121102_0001.
  fits') as f:
4     # File structure information.
5     f.info()
6
7     # f[1].header: observation parameters
8     print("\nTime per bin or sample: {}".format(
9         f[1].header['TBIN']))
10    print("Time sampling points.: {} * {}".
11        format(f[1].header['NAXIS2'], f[1].header['
12            NSBLK']))
13    print("Nr of polarisations: {}".format(f
14        [1].header['NPOL']))
15    print("Number of channels/sub-bands in this
16        file: {}".format(f[1].header['NCHAN']))
17
18    # f[1].data: observation data
19    print("\ndata shape: {}".format(f[1].data['
20        DATA'].shape))
21
22    # output:
23    # No.      Name      Ver      Type      Cards
24    Dimensions  Format
25    # 0 PRIMARY          1 PrimaryHDU    59
26    ()
27    # 1 SUBINT          1 BinTableHDU   76
28    60R x 17C [1D, 1D, 1D, 1D, 1D, 1D, 1D, 1
29    E, 1E, 1E, 1E, 1E, 4096E, 4096E, 4096E,
30    4096E, 4194304B]
31    #
32    # Time per bin or sample: 9.8304e-05
33    # Time sampling points.: 60 * 1024
34    # Nr of polarisations: 1
35    # Number of channels/sub-bands in this file
36    : 4096
37    #
38    # data shape: (60, 1024, 1, 4096, 1)

```

C. BASELINE MODELS EXPERIMENTS

The paper has provided a detailed explanation of the pipelines of these two conventional single-pulse search softwares, PRESTO and Heimdall, and machine learning algorithm RaSPDAM. Here, we will provide the commands and parameters executed in our experiments.

C.1. PRESTO

The software repository link for conventional single-pulse search software PRESTO is <https://github.com/scottransom/presto>.

```

1 # RFI Removal
2 rfifind FRB20121102_0001.fits -o test1 -time 1
3
4 # De-dispersion
5 prepsubband -nobary -numout 524288 -nsub 1024 -
  lodm 350.0 -dmstep 1 -numdms 300 -downsamp
  1 -mask test1_rfifind.mask -o
  FRB20121102_0001 FRB20121102_0001.fits
6
7 # Single-pulse Search
8 ls *.dat |xargs -n 408 -P 12 python
  single_pulse_search.py -b -m 2 -t 3.0

```

C.2. *Heimdall*

The software repository link for conventional single-pulse search software Heimdall is <https://sourceforge.net/projects/heimdall-astro/>. We used `your_heimdall`¹² to test Heimdall on our dataset, as Heimdall's source code does not support processing FITS files and requires a file format conversion. `Your_heimdall` can complete such conversion, essentially using Heimdall to process the file.

1

```
2 your_heimdall.py -dm 350 650 -g 0 -f
  FRB20121102_0001.fits
```

C.3. *RaSPDAM*

The RaSPDAM was implemented in Python. The source code and model file can be found in the attachment. The following example demonstrates an evaluation using a FITS file.

```
1
2 python3 slope_detection.py -o results
  FRB20121102_0001.fits
```

D. DATASET POSITIVE SAMPLES PARAMETERS

¹² https://github.com/thebyteproject/your/blob/main/bin/your_heimdall.py

Table 4. Parameters of 600 Positive Samples in Dataset

Burst File Name	Source	MJD	DM (pc cm^{-3})	ToA (s)	FWHM (ms)	Bandwidth (MHz)	Peak Flux Density (Jy)	Fluence (Jy ms)
FRB20121102.0001.fits	FRB20121102	58724.87756	567.3	3.0926	6.13	110	0.012831	0.0787
FRB20121102.0002.fits	FRB20121102	58724.88513	565.1	3.3074	2.83	400	0.26905	0.7614
FRB20121102.0003.fits	FRB20121102	58724.88637	565.8	1.0731	8.51	160	0.00627	0.0534
FRB20121102.0004.fits	FRB20121102	58724.88758	567.6	4.1216	5.49	200	0.01248	0.0685
FRB20121102.0005.fits	FRB20121102	58724.8911	565.8	1.2662	7.99	230	0.00794	0.0635
FRB20121102.0006.fits	FRB20121102	58724.93325	564.1	4.1918	2.01	320	0.0585	0.1176
FRB20121102.0007.fits	FRB20121102	58724.94249	568.1	3.0237	5.41	230	0.01315	0.0711
FRB20121102.0008.fits	FRB20121102	58724.95614	568	3.5371	4.6	190	0.01413	0.065
FRB20121102.0009.fits	FRB20121102	58724.97639	564	4.4543	5.19	190	0.01614	0.0838
FRB20121102.0010.fits	FRB20121102	58725.87599	567.1	1.2409	2.85	250	0.13023	0.3712
FRB20121102.0011.fits	FRB20121102	58725.87621	562.3	0.6020	6.13	210	0.00446	0.0274
FRB20121102.0012.fits	FRB20121102	58725.88178	565.9	0.2708	6.26	290	0.0065	0.0407
FRB20121102.0013.fits	FRB20121102	58725.88564	566	2.0624	3.84	150	0.01454	0.0559
FRB20121102.0014.fits	FRB20121102	58725.88943	564.5	2.0019	2.03	100	0.14407	0.2925
FRB20121102.0015.fits	FRB20121102	58725.89072	566.1	3.2988	4.44	100	0.06265	0.2782
FRB20121102.0016.fits	FRB20121102	58725.89318	564.5	4.3049	3.12	100	0.09759	0.3045
FRB20121102.0017.fits	FRB20121102	58725.89696	559.7	0.4314	3.66	180	0.02089	0.0766
FRB20121102.0018.fits	FRB20121102	58725.89877	568.5	3.3153	8.88	130	0.01146	0.1017
FRB20121102.0019.fits	FRB20121102	58725.90072	566.7	4.4214	4.92	130	0.01306	0.0642
FRB20121102.0020.fits	FRB20121102	58725.91554	568.5	2.9621	5.89	200	0.01822	0.1073
FRB20121102.0021.fits	FRB20121102	58725.91635	566	2.3250	3.38	120	0.0094	0.0318
FRB20121102.0022.fits	FRB20121102	58725.91764	566	3.5363	3.37	105	0.01415	0.0478
FRB20121102.0023.fits	FRB20121102	58725.9189	566	1.7267	3.54	200	0.01022	0.0362
FRB20121102.0024.fits	FRB20121102	58725.92026	566.3	3.3744	1.92	150	0.15473	0.2971
FRB20121102.0025.fits	FRB20121102	58725.92985	563.2	2.0739	4.54	220	0.00919	0.0417
FRB20121102.0026.fits	FRB20121102	58725.93131	567.6	1.3954	7.91	290	0.01508	0.1192
FRB20121102.0027.fits	FRB20121102	58725.93237	566	4.0378	3.81	300	0.01373	0.0523
FRB20121102.0028.fits	FRB20121102	58725.93294	569.4	0.8811	2.72	140	0.0085	0.0231
FRB20121102.0029.fits	FRB20121102	58725.94049	569.4	0.5990	3.52	280	0.01428	0.0503
FRB20121102.0030.fits	FRB20121102	58725.9409	566	3.9965	4.04	180	0.0125	0.0505
FRB20121102.0031.fits	FRB20121102	58725.94223	566	3.0291	2.9	210	0.02341	0.068
FRB20121102.0032.fits	FRB20121102	58725.95399	565.7	4.5690	5.45	200	0.07952	0.4334
FRB20121102.0033.fits	FRB20121102	58725.95541	554.5	1.0340	4.31	160	0.00709	0.0306
FRB20121102.0034.fits	FRB20121102	58725.9566	567	0.0760	3.47	100	0.06263	0.2173
FRB20121102.0035.fits	FRB20121102	58725.9583	569	1.1831	5.89	150	0.05868	0.3456
FRB20121102.0036.fits	FRB20121102	58725.96176	570	1.6019	10.3	100	0.03169	0.3264

Table 4 continued

Table 4 (continued)

Burst File Name	Source	MJD	DM (pc cm ⁻³)	ToA (s)	FWHM (ms)	Bandwidth (MHz)	Peak Flux Density (Jy)	Fluence (Jy ms)
FRB20121102_0037.fits	FRB20121102	58725.96432	565.9	4.2382	9.14	200	0.10011	0.915
FRB20121102_0038.fits	FRB20121102	58725.9665	564.6	2.3964	2.55	300	0.24736	0.6308
FRB20121102_0039.fits	FRB20121102	58725.97352	566	0.3103	4.06	200	0.01802	0.0732
FRB20121102_0040.fits	FRB20121102	58725.97785	566	1.6335	4.03	200	0.01309	0.0527
FRB20121102_0041.fits	FRB20121102	58725.98146	567.9	2.8102	8.52	250	0.03788	0.3227
FRB20121102_0042.fits	FRB20121102	58725.98847	566	2.1579	3.75	100	0.00924	0.0346
FRB20121102_0043.fits	FRB20121102	58725.99225	563.7	0.8485	3.19	140	0.00901	0.0288
FRB20121102_0044.fits	FRB20121102	58725.99259	566	2.7917	2.67	150	0.01783	0.0475
FRB20121102_0045.fits	FRB20121102	58725.99453	563	2.1191	5.33	50	0.04107	0.2189
FRB20121102_0046.fits	FRB20121102	58725.9983	570	0.8389	5.52	100	0.0475	0.2622
FRB20121102_0047.fits	FRB20121102	58726.9185	564.6	3.3889	2.6	200	0.14299	0.3718
FRB20121102_0048.fits	FRB20121102	58726.92158	568.9	4.1755	7.53	170	0.0083	0.0625
FRB20121102_0049.fits	FRB20121102	58726.92408	566.3	0.6134	4.45	330	0.0126	0.0561
FRB20121102_0050.fits	FRB20121102	58726.92772	550.6	2.6145	4.44	65	0.01136	0.0505
FRB20121102_0051.fits	FRB20121102	58726.92802	564.5	3.4432	6.96	120	0.01402	0.0975
FRB20121102_0052.fits	FRB20121102	58726.93712	566	1.4909	2.88	170	0.00732	0.0211
FRB20121102_0053.fits	FRB20121102	58726.94971	565.6	0.7280	4.64	50	0.04632	0.2149
FRB20121102_0054.fits	FRB20121102	58726.96581	566.2	0.5840	3.01	100	0.0511	0.1538
FRB20121102_0055.fits	FRB20121102	58726.96834	567.9	0.0790	5.23	300	0.07034	0.3679
FRB20121102_0056.fits	FRB20121102	58726.99613	568.5	4.2030	3.74	195	0.00414	0.0155
FRB20121102_0057.fits	FRB20121102	58727.00019	566	3.0518	3.85	180	0.00893	0.0343
FRB20121102_0058.fits	FRB20121102	58727.00142	566	3.3179	4.11	100	0.01053	0.0433
FRB20121102_0059.fits	FRB20121102	58727.00404	566	4.4402	3.99	180	0.01041	0.0415
FRB20121102_0060.fits	FRB20121102	58727.00522	569.4	0.9801	3.35	75	0.00256	0.0086
FRB20121102_0061.fits	FRB20121102	58727.01219	568.5	0.2050	7.54	160	0.01059	0.0799
FRB20121102_0062.fits	FRB20121102	58727.01422	566	1.1606	3.72	110	0.01279	0.0476
FRB20121102_0063.fits	FRB20121102	58727.02681	565.7	0.0360	4.75	350	0.10944	0.5198
FRB20121102_0064.fits	FRB20121102	58727.02699	566	0.6551	3.98	250	0.01353	0.0538
FRB20121102_0065.fits	FRB20121102	58727.0296	566	2.8529	3.58	170	0.01324	0.0474
FRB20121102_0066.fits	FRB20121102	58727.04422	566	2.9126	2.1	150	0.01969	0.0413
FRB20121102_0067.fits	FRB20121102	58727.07798	563.2	1.9210	5.23	30	0.0087	0.0455
FRB20121102_0068.fits	FRB20121102	58727.08786	564.5	0.8655	6.56	150	0.01417	0.0929
FRB20121102_0069.fits	FRB20121102	58727.09232	565.8	1.9720	10.94	400	0.04737	0.5182
FRB20121102_0070.fits	FRB20121102	58727.09706	567.6	0.5870	8.82	165	0.00875	0.0772
FRB20121102_0071.fits	FRB20121102	58727.90379	566	1.8139	4.04	460	0.09887	0.3996
FRB20121102_0072.fits	FRB20121102	58727.90656	565	1.7979	4.75	140	0.00606	0.0288
FRB20121102_0073.fits	FRB20121102	58727.91153	567.2	0.3777	2.62	110	0.00483	0.0127
FRB20121102_0074.fits	FRB20121102	58727.91526	567.2	0.2896	8.12	90	0.0048	0.039
FRB20121102_0075.fits	FRB20121102	58727.91574	563.8	2.8607	2.81	300	0.5953	1.6728

Table 4 continued

Table 4 (continued)

Burst File Name	Source	MJD	DM (pc cm^{-3})	ToA (s)	FWHM (ms)	Bandwidth (MHz)	Peak Flux Density (Jy)	Fluence (Jy ms)
FRB20121102_0076.fits	FRB20121102	58727.92178	566	2.8659	3.83	190	0.03688	0.1411
FRB20121102_0077.fits	FRB20121102	58727.92596	561	3.3395	4	170	0.00746	0.0298
FRB20121102_0078.fits	FRB20121102	58727.92854	562.8	1.3202	3.78	100	0.09252	0.3497
FRB20121102_0079.fits	FRB20121102	58727.93819	566	2.6919	4.55	175	0.01228	0.0559
FRB20121102_0080.fits	FRB20121102	58727.95377	564.5	0.2191	3.15	102	0.00722	0.0227
FRB20121102_0081.fits	FRB20121102	58727.9627	569	1.1860	4.03	105	0.01444	0.0582
FRB20121102_0082.fits	FRB20121102	58727.96275	567.6	0.1072	5.46	110	0.00989	0.054
FRB20121102_0083.fits	FRB20121102	58727.96395	566	1.6053	3.13	210	0.01259	0.0394
FRB20121102_0084.fits	FRB20121102	58727.96483	552.4	2.6858	7.35	175	0.00482	0.0354
FRB20121102_0085.fits	FRB20121102	58727.96512	566	1.4534	4.37	130	0.01041	0.0455
FRB20121102_0086.fits	FRB20121102	58727.97165	565.5	0.9240	3.86	200	0.06539	0.2524
FRB20121102_0087.fits	FRB20121102	58727.98961	565.5	2.5525	6.47	350	0.70504	4.5616
FRB20121102_0088.fits	FRB20121102	58727.99693	566.7	1.2139	6.47	130	0.00498	0.0322
FRB20121102_0089.fits	FRB20121102	58727.99986	565.6	3.6556	3.5	50	0.04882	0.1709
FRB20121102_0090.fits	FRB20121102	58728.00245	566.1	2.2279	3.38	200	0.04817	0.1628
FRB20121102_0091.fits	FRB20121102	58728.00686	562.6	2.3000	5.93	400	0.10736	0.6366
FRB20121102_0092.fits	FRB20121102	58728.01267	566.6	2.1056	8.9	100	0.03219	0.2865
FRB20121102_0093.fits	FRB20121102	58728.01462	569	0.1214	5.42	125	0.00457	0.0248
FRB20121102_0094.fits	FRB20121102	58728.02096	565.1	3.4972	3.71	200	0.7118	2.6408
FRB20121102_0095.fits	FRB20121102	58728.02325	563.7	0.4322	6.2	180	0.00949	0.0588
FRB20121102_0096.fits	FRB20121102	58728.0269	558.9	0.4844	8.52	400	0.00169	0.0144
FRB20121102_0097.fits	FRB20121102	58728.05237	566	3.2574	2.9	300	0.0127	0.0369
FRB20121102_0098.fits	FRB20121102	58728.0573	570	2.5815	9.26	250	0.10363	0.9596
FRB20121102_0099.fits	FRB20121102	58728.0691	566	4.1637	3.03	400	0.01095	0.0332
FRB20121102_0100.fits	FRB20121102	58728.07772	567	3.4837	3.53	200	0.09654	0.3408
FRB20121102_0101.fits	FRB20121102	58728.98495	564.3	2.2867	2.69	50	0.08237	0.2216
FRB20121102_0102.fits	FRB20121102	58728.98842	567.2	3.2979	6.04	150	0.08738	0.5278
FRB20121102_0103.fits	FRB20121102	58728.99392	566	4.6156	3.24	200	0.18703	0.606
FRB20121102_0104.fits	FRB20121102	58729.00494	568.3	4.4047	4.41	400	0.0647	0.2853
FRB20121102_0105.fits	FRB20121102	58729.0085	569	0.5212	6.05	50	0.03638	0.2201
FRB20121102_0106.fits	FRB20121102	58729.01463	568	2.3417	4.05	150	0.05107	0.2068
FRB20121102_0107.fits	FRB20121102	58729.01705	564.6	0.2937	2.02	50	0.0867	0.1751
FRB20121102_0108.fits	FRB20121102	58729.01805	564.7	1.9315	2.88	400	0.0101	0.0291
FRB20121102_0109.fits	FRB20121102	58729.01846	563.1	4.4809	2.2	200	0.16156	0.3554
FRB20121102_0110.fits	FRB20121102	58729.02395	565.4	1.2113	3.15	100	0.07467	0.2352
FRB20121102_0111.fits	FRB20121102	58729.02706	565.1	0.1473	5.27	150	0.04704	0.2479
FRB20121102_0112.fits	FRB20121102	58729.04583	566.6	0.5030	6.79	150	0.05874	0.3988
FRB20121102_0113.fits	FRB20121102	58729.04737	563.5	2.5113	2.21	200	0.11853	0.262
FRB20121102_0114.fits	FRB20121102	58729.05123	563.8	3.7266	3.44	300	0.1523	0.5239

Table 4 continued

Table 4 (continued)

Burst File Name	Source	MJD	DM (pc cm^{-3})	ToA (s)	FWHM (ms)	Bandwidth (MHz)	Peak Flux Density (Jy)	Fluence (Jy ms)
FRB20121102_0115.fits	FRB20121102	58729.05518	568.4	1.6226	5.63	200	0.04226	0.2379
FRB20121102_0116.fits	FRB20121102	58729.05609	561.5	3.0189	5.62	190	0.00628	0.0352
FRB20121102_0117.fits	FRB20121102	58729.06361	569.4	2.9349	8.41	150	0.06767	0.5691
FRB20121102_0118.fits	FRB20121102	58729.06916	569.5	3.0995	4.12	150	0.18388	0.7576
FRB20121102_0119.fits	FRB20121102	58729.07307	564.9	3.0734	2.1	300	0.58318	1.2247
FRB20121102_0120.fits	FRB20121102	58730.87132	568.1	3.4382	7.98	100	0.00909	0.0725
FRB20121102_0121.fits	FRB20121102	58730.87347	567	1.2238	6.88	150	0.05711	0.3929
FRB20121102_0122.fits	FRB20121102	58730.88025	569.5	2.2721	8.43	50	0.0387	0.3262
FRB20121102_0123.fits	FRB20121102	58730.88097	568.1	1.6585	1.79	200	0.00723	0.0129
FRB20121102_0124.fits	FRB20121102	58730.89092	568.9	1.0673	10.11	200	0.04934	0.4988
FRB20121102_0125.fits	FRB20121102	58730.89453	566.9	0.5608	3.56	250	0.10085	0.359
FRB20121102_0126.fits	FRB20121102	58730.90048	566.2	0.6540	4.05	250	0.10584	0.4287
FRB20121102_0127.fits	FRB20121102	58730.90213	567	1.5877	4.89	400	0.07947	0.3886
FRB20121102_0128.fits	FRB20121102	58730.90753	563.6	4.1419	2.71	200	0.44693	1.2112
FRB20121102_0129.fits	FRB20121102	58730.90783	566.9	1.9505	7.29	200	0.04506	0.3285
FRB20121102_0130.fits	FRB20121102	58732.86875	562.8	1.1306	5.94	90	0.00696	0.0414
FRB20121102_0131.fits	FRB20121102	58732.8689	566	2.2367	3.76	170	0.01011	0.0381
FRB20121102_0132.fits	FRB20121102	58732.87047	566	2.1816	3.54	170	0.01775	0.0627
FRB20121102_0133.fits	FRB20121102	58732.87607	566	0.7087	3.13	105	0.0186	0.0582
FRB20121102_0134.fits	FRB20121102	58732.87836	563.7	2.3886	7.2	80	0.00608	0.0438
FRB20121102_0135.fits	FRB20121102	58732.87877	569.4	1.6878	8.56	140	0.00898	0.0768
FRB20121102_0136.fits	FRB20121102	58732.95231	565.9	1.0176	7.53	130	0.00778	0.0586
FRB20121102_0137.fits	FRB20121102	58732.95423	566.7	0.0672	2.96	110	0.00692	0.0205
FRB20121102_0138.fits	FRB20121102	58732.95433	564.1	0.6848	5.71	200	0.00954	0.0544
FRB20121102_0139.fits	FRB20121102	58732.95621	566	2.9801	2.36	130	0.01475	0.0348
FRB20121102_0140.fits	FRB20121102	58732.95934	567.2	2.5572	7.3	160	0.00721	0.0526
FRB20121102_0141.fits	FRB20121102	58732.96003	568.4	3.8131	4.81	100	0.08157	0.3924
FRB20121102_0142.fits	FRB20121102	58732.96073	565.4	0.5333	3.53	120	0.01096	0.0387
FRB20121102_0143.fits	FRB20121102	58732.96268	565.4	0.0903	4.14	210	0.39424	1.6337
FRB20121102_0144.fits	FRB20121102	58732.96286	566	3.9247	2.83	130	0.01545	0.0437
FRB20121102_0145.fits	FRB20121102	58732.96467	567.6	3.1886	4.18	100	0.00914	0.0382
FRB20121102_0146.fits	FRB20121102	58732.96766	566	3.0219	4.61	160	0.01191	0.0549
FRB20121102_0147.fits	FRB20121102	58732.9727	566	4.0211	3.17	30	0.01006	0.0319
FRB20121102_0148.fits	FRB20121102	58732.9731	566	0.3464	1.85	120	0.01839	0.034
FRB20121102_0149.fits	FRB20121102	58732.97436	566	1.0993	2.18	140	0.01223	0.0266
FRB20121102_0150.fits	FRB20121102	58732.97558	566	1.2829	4.04	130	0.01217	0.0492
FRB20121102_0151.fits	FRB20121102	58732.97641	565	2.6086	6.6	130	0.00957	0.0632
FRB20121102_0152.fits	FRB20121102	58732.97759	567.2	0.8794	78.52	170	0.00999	0.7844
FRB20121102_0153.fits	FRB20121102	58732.97994	567.3	4.2107	6.15	250	0.0741	0.4557

Table 4 continued

Table 4 (continued)

Burst File Name	Source	MJD	DM (pc cm^{-3})	ToA (s)	FWHM (ms)	Bandwidth (MHz)	Peak Flux Density (Jy)	Fluence (Jy ms)
FRB20121102_0154.fits	FRB20121102	58732.98207	566	1.4323	3.73	260	0.01173	0.0438
FRB20121102_0155.fits	FRB20121102	58732.98576	567.2	4.1596	3.29	100	0.06227	0.2049
FRB20121102_0156.fits	FRB20121102	58732.98655	559.7	0.9680	2.4	70	0.00519	0.0125
FRB20121102_0157.fits	FRB20121102	58732.99195	565.4	0.6422	7.54	90	0.00767	0.0579
FRB20121102_0158.fits	FRB20121102	58733.90523	564.5	0.4174	2.67	400	0.84239	2.2492
FRB20121102_0159.fits	FRB20121102	58733.91736	565.9	4.3268	0.34	105	0.00474	0.0016
FRB20121102_0160.fits	FRB20121102	58733.91851	566.1	3.6670	2.65	100	0.07565	0.2005
FRB20121102_0161.fits	FRB20121102	58733.91876	567.9	0.0511	5.55	250	0.06527	0.3623
FRB20121102_0162.fits	FRB20121102	58733.91948	565.5	3.3249	2.26	120	0.09033	0.2042
FRB20121102_0163.fits	FRB20121102	58733.92254	562.6	2.9314	1.08	50	0.0421	0.0455
FRB20121102_0164.fits	FRB20121102	58733.92316	564.2	0.4492	1.83	100	0.07733	0.1415
FRB20121102_0165.fits	FRB20121102	58733.93106	566	3.2304	3.94	180	0.00841	0.0331
FRB20121102_0166.fits	FRB20121102	58733.93123	565.6	0.0597	4.61	70	0.01811	0.0836
FRB20121102_0167.fits	FRB20121102	58735.01934	564.4	3.1493	5.92	200	0.07251	0.4293
FRB20121102_0168.fits	FRB20121102	58735.02504	568.4	4.4950	3.66	230	0.05453	0.1996
FRB20121102_0169.fits	FRB20121102	58735.02663	566.7	0.9791	21.27	400	0.0311	0.6615
FRB20121102_0170.fits	FRB20121102	58735.02707	563.9	0.4344	2.58	350	0.67999	1.7544
FRB20121102_0171.fits	FRB20121102	58735.02846	566.1	0.6257	5.38	180	0.08944	0.4812
FRB20121102_0172.fits	FRB20121102	58735.02903	562.8	2.6206	6.74	130	0.00745	0.0502
FRB20121102_0173.fits	FRB20121102	58735.03188	562.6	3.5275	1.99	100	0.09554	0.1901
FRB20121102_0174.fits	FRB20121102	58735.03225	567.6	3.0726	4.07	150	0.09726	0.3959
FRB20121102_0175.fits	FRB20121102	58735.03723	567.4	2.1610	5.02	200	0.07755	0.3893
FRB20121102_0176.fits	FRB20121102	58735.04017	566.5	4.0428	4.49	300	0.06999	0.3143
FRB20121102_0177.fits	FRB20121102	58735.04043	568.3	2.0596	11.01	300	0.04435	0.4883
FRB20121102_0178.fits	FRB20121102	58735.04416	563	4.6303	3.71	250	0.09052	0.3358
FRB20121102_0179.fits	FRB20121102	58735.04608	565	3.2099	7.5	132	0.00654	0.0491
FRB20121102_0180.fits	FRB20121102	58736.96951	569.5	2.4488	8.85	110	0.04439	0.3929
FRB20121102_0181.fits	FRB20121102	58736.97536	566.5	0.9557	4.58	450	0.04668	0.2138
FRB20121102_0182.fits	FRB20121102	58736.98094	564.3	4.4411	2.86	300	0.32433	0.9276
FRB20121102_0183.fits	FRB20121102	58736.98189	567.2	1.6646	7.33	400	0.04762	0.3491
FRB20121102_0184.fits	FRB20121102	58736.98387	566.7	0.6317	4.19	120	0.05879	0.2463
FRB20121102_0185.fits	FRB20121102	58736.98432	566.7	3.0716	7.06	150	0.05033	0.3553
FRB20121102_0186.fits	FRB20121102	58736.98563	567.7	1.6761	5.03	250	0.04024	0.2024
FRB20121102_0187.fits	FRB20121102	58736.98838	569.8	0.9442	6.87	100	0.04001	0.2749
FRB20121102_0188.fits	FRB20121102	58736.99206	563.6	3.8486	3.52	350	0.13712	0.4827
FRB20121102_0189.fits	FRB20121102	58736.99293	563.5	0.3799	2.99	150	0.08017	0.2397
FRB20121102_0190.fits	FRB20121102	58738.95952	566	3.9626	4.49	200	0.01015	0.0456
FRB20121102_0191.fits	FRB20121102	58738.96014	559.7	1.9365	6.61	170	0.0104	0.0688
FRB20121102_0192.fits	FRB20121102	58738.96335	565.8	0.2539	3.95	50	0.00681	0.0269

Table 4 continued

Table 4 (continued)

Burst File Name	Source	MJD	DM (pc cm^{-3})	ToA (s)	FWHM (ms)	Bandwidth (MHz)	Peak Flux Density (Jy)	Fluence (Jy ms)
FRB20121102_0193.fits	FRB20121102	58738.96367	565.8	1.1001	5.77	50	0.00734	0.0424
FRB20121102_0194.fits	FRB20121102	58738.96742	567.1	1.5596	8.61	100	0.00453	0.039
FRB20121102_0195.fits	FRB20121102	58738.96876	565.1	1.0335	6.79	50	0.00912	0.0619
FRB20121102_0196.fits	FRB20121102	58738.97076	568.5	4.2439	3.45	50	0.0077	0.0266
FRB20121102_0197.fits	FRB20121102	58738.97434	564.8	4.4162	4.06	200	0.00792	0.0322
FRB20121102_0198.fits	FRB20121102	58738.97624	564.9	2.5251	1.91	50	0.01044	0.0199
FRB20121102_0199.fits	FRB20121102	58738.97667	563.8	2.5964	2.84	50	0.0079	0.0224
FRB20121102_0200.fits	FRB20121102	58738.97741	566.1	0.7432	5.51	50	0.0093	0.0512
FRB20121102_0201.fits	FRB20121102	58738.97778	565.5	0.5270	0.5	100	0.0095	0.0048
FRB20121102_0202.fits	FRB20121102	58738.97869	566.4	0.1743	5.32	150	0.01406	0.0748
FRB20121102_0203.fits	FRB20121102	58738.98134	567.9	3.5519	3.63	100	0.01496	0.0543
FRB20121102_0204.fits	FRB20121102	58738.9872	565.2	1.0840	7.34	150	0.00843	0.0619
FRB20121102_0205.fits	FRB20121102	58738.98816	565.5	1.7002	8.47	150	0.00545	0.0462
FRB20121102_0206.fits	FRB20121102	58738.9891	566.4	3.8809	2.46	200	0.0073	0.018
FRB20121102_0207.fits	FRB20121102	58738.98977	566.8	3.2075	7	50	0.00687	0.0481
FRB20121102_0208.fits	FRB20121102	58738.9902	569.3	0.5342	6.05	50	0.00709	0.0429
FRB20121102_0209.fits	FRB20121102	58738.99141	568.3	0.1097	8.1	180	0.01024	0.0829
FRB20121102_0210.fits	FRB20121102	58738.995	566.7	1.5651	3.69	100	0.00457	0.0169
FRB20121102_0211.fits	FRB20121102	58741.87871	565.7	0.1428	2.82	400	0.01089	0.0307
FRB20121102_0212.fits	FRB20121102	58741.89634	566.1	4.2045	2.12	300	0.18462	0.3914
FRB20121102_0213.fits	FRB20121102	58742.89231	565.6	0.9329	8.39	100	0.00624	0.0524
FRB20121102_0214.fits	FRB20121102	58742.90336	564.5	1.0690	4.21	105	0.0044	0.0185
FRB20121102_0215.fits	FRB20121102	58743.92509	562.8	3.3248	3.94	100	0.01634	0.0644
FRB20121102_0216.fits	FRB20121102	58743.92581	566.5	0.7273	6.2	150	0.00954	0.0592
FRB20121102_0217.fits	FRB20121102	58743.9406	566.6	1.4758	3.14	150	0.01919	0.0603
FRB20121102_0218.fits	FRB20121102	58743.94263	564.1	1.9594	4.1	400	0.01628	0.0668
FRB20121102_0219.fits	FRB20121102	58744.87502	566	3.3659	4.77	140	0.01329	0.0633
FRB20121102_0220.fits	FRB20121102	58744.88425	566	2.7010	3.92	120	0.00631	0.0247
FRB20121102_0221.fits	FRB20121102	58744.89612	566	0.6872	2.84	80	0.0208	0.0591
FRB20121102_0222.fits	FRB20121102	58744.90237	566.3	1.5909	6.58	340	0.00907	0.0597
FRB20121102_0223.fits	FRB20121102	58745.93086	567.7	0.5357	4.22	50	0.00805	0.034
FRB20121102_0224.fits	FRB20121102	58745.93325	566.4	0.9162	6.4	100	0.00688	0.044
FRB20121102_0225.fits	FRB20121102	58745.93452	566.7	1.8966	3.52	100	0.00743	0.0262
FRB20121102_0226.fits	FRB20121102	58745.93759	566	2.7633	3.72	100	0.00965	0.0359
FRB20121102_0227.fits	FRB20121102	58745.9404	569	4.4028	3.25	100	0.00748	0.0243
FRB20121102_0228.fits	FRB20121102	58745.94174	566.2	1.3921	5.21	100	0.00895	0.0466
FRB20121102_0229.fits	FRB20121102	58745.94395	568.2	2.7188	9.99	100	0.0052	0.052
FRB20121102_0230.fits	FRB20121102	58745.94534	563.4	4.3974	2.66	60	0.02165	0.0576
FRB20121102_0231.fits	FRB20121102	58745.94721	567.2	2.9940	2.58	50	0.01108	0.0286

Table 4 continued

Table 4 (continued)

Burst File Name	Source	MJD	DM (pc cm ⁻³)	ToA (s)	FWHM (ms)	Bandwidth (MHz)	Peak Flux Density (Jy)	Fluence (Jy ms)
FRB20121102_0232.fits	FRB20121102	58745.9476	566.9	4.4542	7.93	100	0.00538	0.0427
FRB20121102_0233.fits	FRB20121102	58745.94768	566.2	1.9311	3.35	45	0.00975	0.0327
FRB20121102_0234.fits	FRB20121102	58745.95058	564.9	3.9395	5.05	300	0.0076	0.0384
FRB20121102_0235.fits	FRB20121102	58745.95123	565.3	2.4797	10.27	200	0.00768	0.0789
FRB20121102_0236.fits	FRB20121102	58745.96002	567.5	1.2064	5.68	100	0.01042	0.0592
FRB20121102_0237.fits	FRB20121102	58745.96086	566	4.2464	9.55	100	0.00507	0.0484
FRB20121102_0238.fits	FRB20121102	58745.96216	565.3	2.4716	4.26	200	0.00936	0.0399
FRB20121102_0239.fits	FRB20121102	58745.96553	565	1.8612	3.62	80	0.01498	0.0542
FRB20121102_0240.fits	FRB20121102	58746.86415	568.7	4.1699	5.08	100	0.01205	0.0612
FRB20121102_0241.fits	FRB20121102	58746.86959	567	2.7811	11.49	400	0.02209	0.2538
FRB20121102_0242.fits	FRB20121102	58746.86982	567	2.8310	6.83	400	0.02287	0.1562
FRB20121102_0243.fits	FRB20121102	58746.86996	568	2.6960	7.75	50	0.00832	0.0645
FRB20121102_0244.fits	FRB20121102	58746.87026	565.5	2.5361	4.96	150	0.00965	0.0479
FRB20121102_0245.fits	FRB20121102	58746.87225	568.2	1.2516	3.84	100	0.01288	0.0495
FRB20121102_0246.fits	FRB20121102	58746.87421	567.2	1.2864	3.3	100	0.02187	0.0722
FRB20121102_0247.fits	FRB20121102	58746.87676	565.4	3.2958	3.75	150	0.01582	0.0593
FRB20121102_0248.fits	FRB20121102	58746.88144	565.9	2.8998	5.67	100	0.00553	0.0314
FRB20121102_0249.fits	FRB20121102	58746.88301	562.9	2.9836	2.81	300	0.02487	0.0699
FRB20121102_0250.fits	FRB20121102	58746.88367	567.8	1.6313	3	34	0.00866	0.026
FRB20121102_0251.fits	FRB20121102	58746.88573	566.5	0.7936	4.92	150	0.00758	0.0373
FRB20121102_0252.fits	FRB20121102	58746.88867	566.7	2.2947	6.28	400	0.02551	0.1602
FRB20121102_0253.fits	FRB20121102	58746.89303	563.6	1.1133	2.95	50	0.0141	0.0416
FRB20121102_0254.fits	FRB20121102	58746.89315	566.3	1.7203	6.65	200	0.00297	0.0198
FRB20121102_0255.fits	FRB20121102	58746.89415	567.2	4.5206	5.3	100	0.00696	0.0369
FRB20121102_0256.fits	FRB20121102	58746.89449	564.7	0.7122	3.99	200	0.0228	0.091
FRB20121102_0257.fits	FRB20121102	58746.89593	565.3	1.7717	2.58	300	0.06111	0.1577
FRB20121102_0258.fits	FRB20121102	58746.90256	566	4.1600	3.83	210	0.02015	0.0772
FRB20121102_0259.fits	FRB20121102	58747.84599	564.9	3.0805	9.59	200	0.00581	0.0557
FRB20121102_0260.fits	FRB20121102	58747.8464	570	4.2509	4.8	100	0.00778	0.0373
FRB20121102_0261.fits	FRB20121102	58747.8485	565	3.1415	3.52	100	0.02112	0.0743
FRB20121102_0262.fits	FRB20121102	58747.85584	565.4	0.8774	7.75	50	0.00664	0.0515
FRB20121102_0263.fits	FRB20121102	58747.86076	565.4	1.0834	4.49	200	0.01246	0.056
FRB20121102_0264.fits	FRB20121102	58747.86215	565.8	2.8307	2.32	150	0.01034	0.024
FRB20121102_0265.fits	FRB20121102	58747.86471	565.6	2.6456	6.74	170	0.01141	0.0769
FRB20121102_0266.fits	FRB20121102	58747.8657	564.8	2.0373	4.73	185	0.00681	0.0322
FRB20121102_0267.fits	FRB20121102	58747.86672	566.7	0.5945	4.03	150	0.00853	0.0344
FRB20121102_0268.fits	FRB20121102	58748.91222	566	3.3601	3.59	150	0.01846	0.0663
FRB20121102_0269.fits	FRB20121102	58748.92565	565.3	2.4040	5.36	150	0.00524	0.0281
FRB20121102_0270.fits	FRB20121102	58748.92664	567.2	1.7501	6.31	160	0.00661	0.0417

Table 4 continued

Table 4 (continued)

Burst File Name	Source	MJD	DM (pc cm^{-3})	ToA (s)	FWHM (ms)	Bandwidth (MHz)	Peak Flux Density (Jy)	Fluence (Jy ms)
FRB20121102_0271.fits	FRB20121102	58748.93031	564.9	3.8434	2.47	100	0.00827	0.0204
FRB20121102_0272.fits	FRB20121102	58748.93052	566.3	2.9110	3.2	150	0.00257	0.0082
FRB20121102_0273.fits	FRB20121102	58748.93164	569.4	3.1893	4.88	200	0.00843	0.0411
FRB20121102_0274.fits	FRB20121102	58748.93784	566.2	4.1185	4.98	120	0.00793	0.0395
FRB20121102_0275.fits	FRB20121102	58748.93845	566	0.5550	2.49	110	0.01926	0.0479
FRB20121102_0276.fits	FRB20121102	58748.93893	563.7	1.3249	4.47	120	0.00624	0.0279
FRB20121102_0277.fits	FRB20121102	58748.93979	566	2.8377	2.4	110	0.04783	0.1147
FRB20121102_0278.fits	FRB20121102	58748.94589	564.5	1.9318	9.65	280	0.00891	0.086
FRB20121102_0279.fits	FRB20121102	58748.94679	566	1.9071	4.44	180	0.01706	0.0757
FRB20121102_0280.fits	FRB20121102	58748.9474	568.5	0.8342	9.55	105	0.0081	0.0774
FRB20121102_0281.fits	FRB20121102	58748.94759	565.4	1.8548	5.53	100	0.00379	0.021
FRB20121102_0282.fits	FRB20121102	58748.94886	566	3.1757	4.69	90	0.01062	0.0498
FRB20121102_0283.fits	FRB20121102	58748.94931	565.4	2.5971	4.8	110	0.01007	0.0484
FRB20121102_0284.fits	FRB20121102	58748.94983	567.6	2.5732	7.27	110	0.0109	0.0793
FRB20121102_0285.fits	FRB20121102	58748.95086	566	1.2869	3.14	90	0.00816	0.0256
FRB20121102_0286.fits	FRB20121102	58749.86271	567.9	2.1985	8.35	100	0.00701	0.0585
FRB20121102_0287.fits	FRB20121102	58749.86427	566.9	0.3818	4.72	60	0.00871	0.0411
FRB20121102_0288.fits	FRB20121102	58749.86661	567.8	4.2271	2.53	300	0.01515	0.0383
FRB20121102_0289.fits	FRB20121102	58749.86779	566.7	4.6022	6.25	120	0.00784	0.049
FRB20121102_0290.fits	FRB20121102	58749.86804	565.4	2.7366	3.07	100	0.00683	0.021
FRB20121102_0291.fits	FRB20121102	58749.87475	565	3.0190	3.16	200	0.01654	0.0523
FRB20121102_0292.fits	FRB20121102	58749.87518	563.6	3.3339	3.37	50	0.00864	0.0291
FRB20121102_0293.fits	FRB20121102	58749.87747	566	1.5592	5.22	400	0.01981	0.1034
FRB20121102_0294.fits	FRB20121102	58749.87913	567.9	3.2713	7.07	100	0.0086	0.0608
FRB20121102_0295.fits	FRB20121102	58749.87979	567.1	2.9559	5.47	100	0.01133	0.062
FRB20121102_0296.fits	FRB20121102	58749.88282	566.9	2.3244	6.28	200	0.01118	0.0702
FRB20121102_0297.fits	FRB20121102	58749.89254	565.9	2.0921	3.48	140	0.0139	0.0484
FRB20121102_0298.fits	FRB20121102	58750.85696	566	4.3124	2.83	260	0.05948	0.1681
FRB20121102_0299.fits	FRB20121102	58750.85718	568.5	0.2389	4.6	300	0.01501	0.0691
FRB20121102_0300.fits	FRB20121102	58750.8574	568.5	2.4625	4.98	110	0.00583	0.029
FRB20121102_0301.fits	FRB20121102	58750.85948	563.7	1.4771	2.64	50	0.01881	0.0497
FRB20121102_0302.fits	FRB20121102	58750.86107	564.3	1.0863	5.21	40	0.00993	0.0517
FRB20121102_0303.fits	FRB20121102	58750.86208	562.3	3.6439	2.18	220	0.01152	0.0251
FRB20121102_0304.fits	FRB20121102	58750.86531	564.6	0.1207	5.54	400	0.02533	0.1403
FRB20121102_0305.fits	FRB20121102	58750.86659	566.2	1.0208	8.54	300	0.00772	0.0659
FRB20121102_0306.fits	FRB20121102	58750.87267	566.3	4.1655	2.21	130	0.01079	0.0239
FRB20121102_0307.fits	FRB20121102	58750.87588	563.3	3.6707	4.87	120	0.00965	0.047
FRB20121102_0308.fits	FRB20121102	58750.88589	566.3	0.8042	10.96	180	0.00374	0.041
FRB20121102_0309.fits	FRB20121102	58750.88627	569.8	0.6116	8.86	100	0.00576	0.051

Table 4 continued

Table 4 (continued)

Burst File Name	Source	MJD	DM (pc cm^{-3})	ToA (s)	FWHM (ms)	Bandwidth (MHz)	Peak Flux Density (Jy)	Fluence (Jy ms)
FRB20121102_0310.fits	FRB20121102	58750.89113	568.8	4.4651	61.56	50	0.01799	1.1075
FRB20121102_0311.fits	FRB20121102	58750.89601	566	0.1052	4.02	110	0.00847	0.034
FRB20121102_0312.fits	FRB20121102	58750.89622	568.9	2.8886	10.1	170	0.01038	0.1048
FRB20121102_0313.fits	FRB20121102	58750.89645	566	0.9421	2.78	280	0.02297	0.064
FRB20121102_0314.fits	FRB20121102	58751.88605	565.3	4.3767	2.56	200	0.04741	0.1214
FRB20121102_0315.fits	FRB20121102	58751.88985	566.2	1.3331	8.05	50	0.00778	0.0626
FRB20121102_0316.fits	FRB20121102	58751.89606	566	2.7540	3.65	110	0.00747	0.0273
FRB20121102_0317.fits	FRB20121102	58751.89787	565.3	4.4191	4.98	150	0.01258	0.0627
FRB20121102_0318.fits	FRB20121102	58751.90404	566	1.3377	4.5	100	0.01	0.045
FRB20121102_0319.fits	FRB20121102	58751.90431	567.2	0.6525	2.43	100	0.00525	0.0128
FRB20121102_0320.fits	FRB20121102	58751.90735	566	0.4023	6.15	50	0.00723	0.0445
FRB20121102_0321.fits	FRB20121102	58751.90993	561.5	3.2675	7.15	100	0.00493	0.0353
FRB20121102_0322.fits	FRB20121102	58751.91079	564.4	4.4307	3.36	100	0.01186	0.0399
FRB20121102_0323.fits	FRB20121102	58751.91109	564.4	3.8606	4.41	50	0.0064	0.0282
FRB20121102_0324.fits	FRB20121102	58751.91376	564.5	1.0664	3.57	400	0.0117	0.0418
FRB20121102_0325.fits	FRB20121102	58751.91945	566.1	2.2207	6.39	130	0.00752	0.0481
FRB20121102_0326.fits	FRB20121102	58751.9208	565.1	4.1069	5.94	300	0.00695	0.0413
FRB20121102_0327.fits	FRB20121102	58752.85282	564.2	0.4876	4.25	250	0.00961	0.0408
FRB20121102_0328.fits	FRB20121102	58752.8536	567.4	1.7484	2.16	300	0.07684	0.166
FRB20121102_0329.fits	FRB20121102	58752.85522	555.4	0.6615	7.08	105	0.00308	0.0218
FRB20121102_0330.fits	FRB20121102	58752.856	561.5	2.0174	6.57	150	0.00604	0.0396
FRB20121102_0331.fits	FRB20121102	58752.85948	565.1	2.1707	7.98	50	0.00731	0.0583
FRB20121102_0332.fits	FRB20121102	58752.86034	563.7	4.5954	5.25	220	0.00988	0.0519
FRB20121102_0333.fits	FRB20121102	58752.86209	566.6	2.1716	6.27	200	0.00877	0.055
FRB20121102_0334.fits	FRB20121102	58752.87052	567.3	2.5578	4.59	250	0.01508	0.0692
FRB20121102_0335.fits	FRB20121102	58752.87064	566.5	1.0909	3.5	270	0.05108	0.1783
FRB20121102_0336.fits	FRB20121102	58752.87338	567.4	4.4617	4.71	200	0.01145	0.0539
FRB20121102_0337.fits	FRB20121102	58752.87364	565.9	1.5629	1.37	100	0.02034	0.0279
FRB20121102_0338.fits	FRB20121102	58752.87378	565.7	2.1806	7.16	150	0.00668	0.0478
FRB20121102_0339.fits	FRB20121102	58752.87885	566.4	2.1252	3.12	140	0.02886	0.09
FRB20121102_0340.fits	FRB20121102	58752.88116	568	0.2969	3.11	450	0.04004	0.1245
FRB20121102_0341.fits	FRB20121102	58752.88414	565.2	0.5628	4.48	50	0.00932	0.0418
FRB20121102_0342.fits	FRB20121102	58752.88665	564.3	4.4592	3.15	150	0.02319	0.0731
FRB20121102_0343.fits	FRB20121102	58752.88687	564.4	1.8776	2.6	220	0.01093	0.0284
FRB20121102_0344.fits	FRB20121102	58752.88698	564.3	0.7456	4.6	150	0.01118	0.0514
FRB20121102_0345.fits	FRB20121102	58752.88846	563.4	0.0097	9.9	400	0.00692	0.0685
FRB20121102_0346.fits	FRB20121102	58753.92768	567.4	1.2670	5.53	70	0.00476	0.0263
FRB20121102_0347.fits	FRB20121102	58753.93059	567.1	1.0614	3.92	200	0.01035	0.0406
FRB20121102_0348.fits	FRB20121102	58753.93068	567.9	3.6089	3.5	200	0.01502	0.0526

Table 4 continued

Table 4 (continued)

Burst File Name	Source	MJD	DM (pc cm^{-3})	ToA (s)	FWHM (ms)	Bandwidth (MHz)	Peak Flux Density (Jy)	Fluence (Jy ms)
FRB20121102_0349.fits	FRB20121102	58753.93376	564.7	0.6172	3.39	160	0.00872	0.0296
FRB20121102_0350.fits	FRB20121102	58753.93442	569.3	3.6864	3.28	310	0.0089	0.0292
FRB20121102_0351.fits	FRB20121102	58753.93798	567.7	1.6588	3.26	120	0.00725	0.0236
FRB20121102_0352.fits	FRB20121102	58753.93928	567.8	1.1772	2.87	100	0.00861	0.0247
FRB20121102_0353.fits	FRB20121102	58753.94079	567.1	0.9669	7.44	120	0.0097	0.0722
FRB20121102_0354.fits	FRB20121102	58753.94112	562.9	2.3158	4.81	300	0.02063	0.0992
FRB20121102_0355.fits	FRB20121102	58753.94543	568	3.9236	2.1	80	0.01031	0.0217
FRB20121102_0356.fits	FRB20121102	58753.94629	568.1	0.9342	8.06	110	0.0048	0.0387
FRB20121102_0357.fits	FRB20121102	58753.94928	567.6	0.5815	2.28	40	0.01055	0.0241
FRB20121102_0358.fits	FRB20121102	58753.95238	565.1	1.3091	7.42	120	0.00947	0.0703
FRB20121102_0359.fits	FRB20121102	58754.98428	566	0.4893	3.49	160	0.02719	0.0949
FRB20121102_0360.fits	FRB20121102	58754.98708	569.2	1.2337	3.92	400	0.00849	0.0333
FRB20121102_0361.fits	FRB20121102	58754.99056	566.7	3.5296	3.59	60	0.01438	0.0516
FRB20121102_0362.fits	FRB20121102	58754.99907	568.1	4.2860	3.82	150	0.01289	0.0492
FRB20121102_0363.fits	FRB20121102	58754.99448	566.5	2.3784	1.57	360	0.01269	0.0199
FRB20121102_0364.fits	FRB20121102	58754.99514	564.9	1.6690	3.13	130	0.0135	0.0423
FRB20121102_0365.fits	FRB20121102	58754.99724	566.7	1.6437	3.28	400	0.01878	0.0616
FRB20121102_0366.fits	FRB20121102	58754.99752	566.4	0.6105	4.1	150	0.01145	0.0469
FRB20121102_0367.fits	FRB20121102	58755.00473	561.9	1.6620	6.03	200	0.00465	0.028
FRB20121102_0368.fits	FRB20121102	58755.00658	565.7	4.1140	3.45	100	0.01029	0.0355
FRB20121102_0369.fits	FRB20121102	58755.00686	565.2	2.4115	6.22	45	0.00663	0.0412
FRB20121102_0370.fits	FRB20121102	58755.01388	568.1	1.1213	2.3	120	0.01525	0.0351
FRB20121102_0371.fits	FRB20121102	58755.01393	568.5	0.4012	4.39	300	0.00512	0.0225
FRB20121102_0372.fits	FRB20121102	58755.01441	566.3	1.0636	4.05	100	0.00933	0.0378
FRB20121102_0373.fits	FRB20121102	58755.01841	564.7	3.8394	2.64	190	0.01624	0.0429
FRB20121102_0374.fits	FRB20121102	58755.02051	569.2	4.6207	5.34	200	0.01689	0.0902
FRB20121102_0375.fits	FRB20121102	58755.02213	566.2	2.9072	3.55	150	0.02077	0.0737
FRB20121102_0376.fits	FRB20121102	58755.0229	564.4	0.5027	3.15	115	0.01611	0.0508
FRB20121102_0377.fits	FRB20121102	58755.02339	566	0.2776	3.63	240	0.02006	0.0728
FRB20121102_0378.fits	FRB20121102	58756.84317	566	1.1739	2.6	220	0.0254	0.066
FRB20121102_0379.fits	FRB20121102	58756.84329	566	2.1476	3.83	170	0.0126	0.0482
FRB20121102_0380.fits	FRB20121102	58756.84702	566.7	1.6581	3.4	90	0.01343	0.0457
FRB20121102_0381.fits	FRB20121102	58756.84872	565.1	0.5683	3.41	40	0.01185	0.0404
FRB20121102_0382.fits	FRB20121102	58756.85209	566.4	1.4503	2.36	60	0.02513	0.0593
FRB20121102_0383.fits	FRB20121102	58756.85277	566.2	4.4169	7.03	80	0.01068	0.0751
FRB20121102_0384.fits	FRB20121102	58756.85514	566	1.9931	4.9	150	0.01239	0.0607
FRB20121102_0385.fits	FRB20121102	58756.85753	566	2.7489	4.06	90	0.00757	0.0307
FRB20121102_0386.fits	FRB20121102	58756.85797	565.1	0.7899	2.21	90	0.01265	0.028
FRB20121102_0387.fits	FRB20121102	58756.8589	565.7	4.5791	2.37	95	0.01006	0.0238

Table 4 continued

Table 4 (continued)

Burst File Name	Source	MJD	DM (pc cm^{-3})	ToA (s)	FWHM (ms)	Bandwidth (MHz)	Peak Flux Density (Jy)	Fluence (Jy ms)
FRB20121102_0388.fits	FRB20121102	58756.85974	564.1	0.9980	5.95	200	0.00393	0.0234
FRB20121102_0389.fits	FRB20121102	58756.86064	566.1	0.4693	4.01	350	0.03101	0.1244
FRB20121102_0390.fits	FRB20121102	58756.86104	567.2	1.7961	12.1	190	0.00493	0.0596
FRB20121102_0391.fits	FRB20121102	58756.86254	566.1	1.5464	3.37	400	0.01625	0.0548
FRB20121102_0392.fits	FRB20121102	58756.86532	567.4	3.9016	7.33	190	0.01535	0.1125
FRB20121102_0393.fits	FRB20121102	58756.86659	567.3	2.0154	3.59	100	0.01446	0.0519
FRB20121102_0394.fits	FRB20121102	58756.8676	567.3	1.5763	3.22	50	0.01418	0.0457
FRB20121102_0395.fits	FRB20121102	58756.86956	564.4	0.9883	3.69	140	0.01275	0.0471
FRB20121102_0396.fits	FRB20121102	58756.87315	567.3	0.4900	5.81	200	0.02111	0.1227
FRB20121102_0397.fits	FRB20121102	58756.87389	565.9	2.8955	9	130	0.00953	0.0858
FRB20121102_0398.fits	FRB20121102	58756.87653	566.7	0.2041	5.49	200	0.00829	0.0455
FRB20121102_0399.fits	FRB20121102	58756.8777	565.8	3.9097	5.02	230	0.01269	0.0637
FRB20121102_0400.fits	FRB20121102	58756.87874	566.7	3.7163	5.31	70	0.00718	0.0381
FRB20121102_0401.fits	FRB20121102	58756.88094	566.4	0.8947	3.33	40	0.01468	0.0489
FRB20121102_0402.fits	FRB20121102	58757.89884	566	2.5113	6.12	140	0.01427	0.0873
FRB20121102_0403.fits	FRB20121102	58757.90141	567	2.7647	6.34	90	0.00453	0.0287
FRB20121102_0404.fits	FRB20121102	58757.90386	566.1	1.3238	2.76	180	0.02629	0.0726
FRB20121102_0405.fits	FRB20121102	58757.90426	566.1	4.0922	3.74	180	0.01182	0.0442
FRB20121102_0406.fits	FRB20121102	58757.90635	565.8	3.1543	2.33	150	0.01611	0.0375
FRB20121102_0407.fits	FRB20121102	58757.91478	564.9	3.7430	5.52	120	0.01112	0.0614
FRB20121102_0408.fits	FRB20121102	58757.91594	561.2	0.0621	3.98	80	0.00924	0.0368
FRB20121102_0409.fits	FRB20121102	58757.91699	567.9	1.1835	5.47	80	0.00807	0.0441
FRB20121102_0410.fits	FRB20121102	58757.91916	565.5	3.6007	19.75	80	0.00488	0.0964
FRB20121102_0411.fits	FRB20121102	58757.91923	566.9	2.0230	5.95	80	0.00734	0.0437
FRB20121102_0412.fits	FRB20121102	58757.91978	564.6	4.2861	4.13	400	0.03347	0.1382
FRB20121102_0413.fits	FRB20121102	58757.92414	568	0.9172	5.99	400	0.0196	0.1174
FRB20121102_0414.fits	FRB20121102	58757.92447	564.9	1.0551	4.98	150	0.00935	0.0466
FRB20121102_0415.fits	FRB20121102	58757.92546	565.4	4.5369	9.2	50	0.00772	0.071
FRB20121102_0416.fits	FRB20121102	58757.92926	565.2	4.1266	3.05	450	0.39712	1.2112
FRB20121102_0417.fits	FRB20121102	58757.92939	568	1.1817	4.68	150	0.00552	0.0258
FRB20121102_0418.fits	FRB20121102	58757.93043	567	0.2854	3.45	300	0.01545	0.0533
FRB20121102_0419.fits	FRB20121102	58757.93107	564.8	2.7428	2.37	180	0.00647	0.0153
FRB20121102_0420.fits	FRB20121102	58757.9339	564.7	1.5820	2.91	190	0.02252	0.0655
FRB20121102_0421.fits	FRB20121102	58757.93409	567.2	3.4956	7.92	115	0.00481	0.0381
FRB20121102_0422.fits	FRB20121102	58758.94171	567.4	4.1971	4.55	180	0.01165	0.053
FRB20121102_0423.fits	FRB20121102	58758.95195	566.1	2.1474	3.46	100	0.00868	0.03
FRB20121102_0424.fits	FRB20121102	58758.9584	565.7	2.7681	1.91	320	0.35048	0.6694
FRB20121102_0425.fits	FRB20121102	58758.95904	566.6	0.3917	4.36	100	0.00758	0.0331
FRB20121102_0426.fits	FRB20121102	58758.95921	567.6	1.9848	1.8	100	0.00715	0.0129

Table 4 continued

Table 4 (continued)

Burst File Name	Source	MJD	DM (pc cm^{-3})	ToA (s)	FWHM (ms)	Bandwidth (MHz)	Peak Flux Density (Jy)	Fluence (Jy ms)
FRB20121102_0427.fits	FRB20121102	58758.96064	567.6	2.9826	9.52	100	0.00741	0.0705
FRB20121102_0428.fits	FRB20121102	58758.96135	566.2	4.3479	7.46	100	0.00878	0.0655
FRB20121102_0429.fits	FRB20121102	58758.96159	566	0.3154	3.19	115	0.00862	0.0275
FRB20121102_0430.fits	FRB20121102	58758.96404	566.2	3.1124	5.15	200	0.01033	0.0532
FRB20121102_0431.fits	FRB20121102	58758.96414	569	2.7000	7.33	85	0.00255	0.0187
FRB20121102_0432.fits	FRB20121102	58758.96667	565.3	2.5687	4.46	150	0.01102	0.0492
FRB20121102_0433.fits	FRB20121102	58758.96702	568	4.4173	6.49	160	0.01055	0.0685
FRB20121102_0434.fits	FRB20121102	58758.97225	567.5	2.4748	3.18	100	0.01006	0.032
FRB20121102_0435.fits	FRB20121102	58758.9751	564.2	2.0651	3.59	200	0.01506	0.0541
FRB20121102_0436.fits	FRB20121102	58758.97645	565.2	2.8060	6.05	280	0.01614	0.0977
FRB20121102_0437.fits	FRB20121102	58759.94262	567.1	0.2339	3.8	300	0.01982	0.0753
FRB20121102_0438.fits	FRB20121102	58759.94449	564.8	4.2899	5.14	400	0.01306	0.0671
FRB20121102_0439.fits	FRB20121102	58759.94491	570	3.6067	3.4	300	0.01185	0.0403
FRB20121102_0440.fits	FRB20121102	58759.94825	566.4	0.6175	3.82	300	0.00911	0.0348
FRB20121102_0441.fits	FRB20121102	58759.94879	564.3	1.9187	2.44	150	0.02549	0.0622
FRB20121102_0442.fits	FRB20121102	58759.95847	567.5	4.1393	4.73	100	0.0086	0.0407
FRB20121102_0443.fits	FRB20121102	58759.95866	570	4.5072	7.89	200	0.00551	0.0435
FRB20121102_0444.fits	FRB20121102	58759.96085	566.2	3.0032	2.69	100	0.01692	0.0455
FRB20121102_0445.fits	FRB20121102	58759.96683	566.5	2.5862	4.92	150	0.01288	0.0634
FRB20121102_0446.fits	FRB20121102	58759.96879	568.9	2.8709	8.35	100	0.00664	0.0554
FRB20121102_0447.fits	FRB20121102	58759.96943	566	0.6424	3.58	105	0.00801	0.0287
FRB20121102_0448.fits	FRB20121102	58759.97445	564.8	3.5696	4.98	110	0.01133	0.0573
FRB20121102_0449.fits	FRB20121102	58762.83727	565.8	2.1320	2.62	300	0.01446	0.0379
FRB20121102_0450.fits	FRB20121102	58762.84622	564.4	0.6566	2.03	370	0.14109	0.2864
FRB20121102_0451.fits	FRB20121102	58762.85632	565.4	1.6781	3.81	250	0.02025	0.0772
FRB20121102_0452.fits	FRB20121102	58763.82415	564.7	1.6423	3.16	120	0.01738	0.0549
FRB20121102_0453.fits	FRB20121102	58763.84299	565.1	2.1008	3.99	100	0.0091	0.0363
FRB20121102_0454.fits	FRB20121102	58766.92944	567.4	3.3591	2.88	130	0.04139	0.1192
FRB20121102_0455.fits	FRB20121102	58766.95707	566.3	0.8734	7	400	0.01963	0.1374
FRB20121102_0456.fits	FRB20121102	58767.95407	565.1	2.5709	3.5	180	0.0135	0.0446
FRB20121102_0457.fits	FRB20121102	58767.96079	564.6	3.2917	3.3	100	0.03825	0.109
FRB20121102_0458.fits	FRB20121102	58767.97573	569.8	1.6591	2.85	80	0.00542	0.0572
FRB20121102_0459.fits	FRB20121102	58768.91171	569.2	0.9173	3.2	70	0.01609	0.0973
FRB20121102_0460.fits	FRB20121102	58768.93974	568	2.8340	3.2	280	0.01921	0.0617
FRB20121102_0461.fits	FRB20121102	58772.90647	563.6	4.0108	2.2	110	0.02732	0.0432
FRB20121102_0462.fits	FRB20121102	58774.92421	566	2.9677	2.44	105	0.0146	0.0356
FRB20121102_0463.fits	FRB20121102	58776.8403	567.4	3.8838	10.71	70	0.00822	0.088
FRB20121102_0464.fits	FRB20121102	58776.84098	564.4	1.2192	5.39	70	0.00777	0.0419
FRB20121102_0465.fits	FRB20121102	58776.84319	564.4	0.5359	2.12	180	0.04351	0.0922

Table 4 continued

Table 4 (continued)

Burst File Name	Source	MJD	DM (pc cm ⁻³)	ToA (s)	FWHM (ms)	Bandwidth (MHz)	Peak Flux Density (Jy)	Fluence (Jy ms)
FRB20121102_0466.fits	FRB20121102	58776.855	565.4	2.9935	6.46	70	0.00731	0.0472
FRB20121102_0467.fits	FRB20121102	58776.86099	564.7	2.3032	2.9	120	0.00743	0.0216
FRB20121102_0468.fits	FRB20121102	58776.87691	565.6	0.8124	2.22	160	0.00933	0.0207
FRB20121102_0469.fits	FRB20121102	58776.87755	567.6	3.5502	7.98	75	0.00932	0.0744
FRB20121102_0470.fits	FRB20121102	58776.87781	566	0.1444	2.58	300	0.04605	0.1119
FRB20180301_0001.fits	FRB20180301	59282.46272	517.8	3.3275	12.3	224	0.079	0.9717
FRB20180301_0002.fits	FRB20180301	59282.51991	517.81	2.4952	4.1	63	0.044	0.1804
FRB20180301_0003.fits	FRB20180301	59282.52654	518	2.2349	1.7	16	0.028	0.0476
FRB20180301_0004.fits	FRB20180301	59292.40703	517.83	1.1086	4.1	107	0.105	0.4305
FRB20180301_0005.fits	FRB20180301	59292.41184	517.9	4.0180	7.9	142	0.06	0.474
FRB20201124_0001.fits	FRB20201124	59482.94673	412.97	2.7003	3.78	150	0.02861	0.108
FRB20201124_0002.fits	FRB20201124	59482.95569	412.97	3.7224	3.71	300	0.0307	0.114
FRB20201124_0003.fits	FRB20201124	59482.95927	412.97	3.5893	6.77	400	0.22702	1.537
FRB20201124_0004.fits	FRB20201124	59482.96238	412.97	2.0929	8.69	250	0.01473	0.128
FRB20201124_0005.fits	FRB20201124	59482.96311	412.97	0.8357	6.23	150	0.01011	0.063
FRB20201124_0006.fits	FRB20201124	59482.96594	412.97	0.4880	9.44	400	0.19332	1.825
FRB20201124_0007.fits	FRB20201124	59482.96783	412.97	3.0348	6.66	150	0.01006	0.067
FRB20201124_0008.fits	FRB20201124	59482.98046	412.97	4.7396	9.6	350	0.38298	3.678
FRB20201124_0009.fits	FRB20201124	59482.98135	412.97	4.7250	5.51	400	0.033	0.182
FRB20201124_0010.fits	FRB20201124	59483.86744	412.18	2.3968	4.14	400	0.03259	0.135
FRB20201124_0011.fits	FRB20201124	59483.8701	412.18	0.5039	7.09	450	0.20731	1.47
FRB20201124_0012.fits	FRB20201124	59483.87224	412.18	4.4801	5.57	350	0.12014	0.669
FRB20201124_0013.fits	FRB20201124	59483.88047	412.18	0.4423	6.46	200	0.01038	0.067
FRB20201124_0014.fits	FRB20201124	59483.8957	412.18	2.7318	4.55	100	0.02306	0.105
FRB20201124_0015.fits	FRB20201124	59483.89627	412.18	0.0612	8.68	150	0.03019	0.262
FRB20201124_0016.fits	FRB20201124	59483.89824	412.18	2.8381	4.04	300	0.05254	0.212
FRB20201124_0017.fits	FRB20201124	59483.8993	412.18	3.9064	4.73	250	0.02074	0.098
FRB20201124_0018.fits	FRB20201124	59484.81554	411.51	1.9948	5.29	200	0.00812	0.043
FRB20201124_0019.fits	FRB20201124	59484.81572	411.51	4.1492	6.33	500	0.10944	0.693
FRB20201124_0020.fits	FRB20201124	59484.8162	411.51	1.3943	4.42	200	0.01493	0.066
FRB20201124_0021.fits	FRB20201124	59484.81856	411.51	4.8243	6.1	400	0.02854	0.174
FRB20201124_0022.fits	FRB20201124	59484.82136	411.51	2.1230	3.59	400	0.22818	0.82
FRB20201124_0023.fits	FRB20201124	59484.82186	411.51	0.5458	8.04	200	0.02936	0.236
FRB20201124_0024.fits	FRB20201124	59484.82265	411.51	4.0536	7.27	300	0.05555	0.404
FRB20201124_0025.fits	FRB20201124	59484.82365	411.51	0.9503	3.06	450	0.0712	0.218
FRB20201124_0026.fits	FRB20201124	59484.82496	411.51	3.7418	2.54	200	0.02521	0.064
FRB20201124_0027.fits	FRB20201124	59484.82808	411.51	2.8847	2.91	200	0.02368	0.069
FRB20201124_0028.fits	FRB20201124	59484.82964	411.51	1.8811	5.92	350	0.08597	0.509
FRB20201124_0029.fits	FRB20201124	59484.83066	411.51	0.8569	7.67	100	0.02593	0.199

Table 4 continued

Table 4 (continued)

Burst File Name	Source	MJD	DM (pc cm^{-3})	ToA (s)	FWHM (ms)	Bandwidth (MHz)	Peak Flux Density (Jy)	Fluence (Jy ms)
FRB20201124_0030.fits	FRB20201124	59484.83135	411.51	2.3560	2.55	200	0.02704	0.069
FRB20201124_0031.fits	FRB20201124	59484.8319	411.51	4.9294	9.63	500	0.35286	3.397
FRB20201124_0032.fits	FRB20201124	59484.83209	411.51	1.5283	3.26	200	0.01195	0.039
FRB20201124_0033.fits	FRB20201124	59484.83249	411.51	3.9447	7.55	300	0.01484	0.112
FRB20201124_0034.fits	FRB20201124	59484.83323	411.51	3.3108	4.48	450	0.33391	1.495
FRB20201124_0035.fits	FRB20201124	59484.83476	411.51	0.8373	7.98	300	0.11472	0.916
FRB20201124_0036.fits	FRB20201124	59484.83525	411.51	3.3689	10.68	500	0.22182	2.263
FRB20201124_0037.fits	FRB20201124	59484.83536	411.51	0.7370	4.42	450	0.68057	3.008
FRB20201124_0038.fits	FRB20201124	59484.83653	411.51	4.9067	8.89	250	0.19766	1.757
FRB20201124_0039.fits	FRB20201124	59484.83697	411.51	4.4501	3.4	150	0.01939	0.066
FRB20201124_0040.fits	FRB20201124	59484.83754	411.51	2.5088	7.05	200	0.01419	0.1
FRB20201124_0041.fits	FRB20201124	59484.8399	411.51	0.3685	5.8	350	0.06	0.348
FRB20201124_0042.fits	FRB20201124	59484.84035	411.51	0.3013	3.53	200	0.03793	0.134
FRB20201124_0043.fits	FRB20201124	59484.8407	411.51	4.8488	4.25	300	0.07298	0.31
FRB20201124_0044.fits	FRB20201124	59484.84085	411.51	4.4124	5.08	400	0.02167	0.11
FRB20201124_0045.fits	FRB20201124	59484.84309	411.51	4.4885	4.69	300	0.01789	0.084
FRB20201124_0046.fits	FRB20201124	59484.84313	411.51	2.4136	6.12	400	0.14354	0.878
FRB20201124_0047.fits	FRB20201124	59484.84336	411.51	2.3310	3.87	150	0.01886	0.073
FRB20201124_0048.fits	FRB20201124	59484.84419	411.51	2.8879	5.84	400	0.42931	2.506
FRB20201124_0049.fits	FRB20201124	59484.84477	411.51	1.7231	4.3	200	0.01024	0.044
FRB20201124_0050.fits	FRB20201124	59484.84612	411.51	2.5106	6.99	400	0.30162	2.108
FRB20201124_0051.fits	FRB20201124	59484.84633	411.51	1.9113	6.4	100	0.02656	0.17
FRB20201124_0052.fits	FRB20201124	59484.84702	411.51	2.9337	5.81	400	0.16846	0.979
FRB20201124_0053.fits	FRB20201124	59484.84806	411.51	2.7883	6.74	200	0.02877	0.194
FRB20201124_0054.fits	FRB20201124	59484.84908	411.51	0.5312	7.28	100	0.01497	0.109
FRB20201124_0055.fits	FRB20201124	59484.84969	411.51	2.2557	3.07	300	0.34016	1.044
FRB20201124_0056.fits	FRB20201124	59484.85013	411.51	1.4663	2.88	250	0.57024	1.642
FRB20201124_0057.fits	FRB20201124	59484.85061	411.51	3.5011	3.04	400	0.40414	1.229
FRB20201124_0058.fits	FRB20201124	59484.85066	411.51	1.8453	13.19	300	0.03708	0.489
FRB20201124_0059.fits	FRB20201124	59484.85253	411.51	2.7848	9.86	400	0.29045	2.865
FRB20201124_0060.fits	FRB20201124	59485.78533	412.55	1.4799	5.73	200	0.03127	0.179
FRB20201124_0061.fits	FRB20201124	59485.78541	412.55	1.9897	4.83	200	0.018	0.087
FRB20201124_0062.fits	FRB20201124	59485.78676	412.55	2.7754	7.21	350	0.0334	0.241
FRB20201124_0063.fits	FRB20201124	59485.7875	412.55	2.6713	3.3	150	0.02272	0.075
FRB20201124_0064.fits	FRB20201124	59485.78764	412.55	1.6791	8.72	350	0.11407	0.995
FRB20201124_0065.fits	FRB20201124	59485.78803	412.55	3.0175	4.16	200	0.09997	0.416
FRB20201124_0066.fits	FRB20201124	59485.78847	412.55	2.1201	5.36	500	0.08858	0.475
FRB20201124_0067.fits	FRB20201124	59485.78854	412.55	2.0278	8.15	500	0.21076	1.718
FRB20201124_0068.fits	FRB20201124	59485.78879	412.55	4.1653	4.88	350	0.02993	0.146

Table 4 continued

Table 4 (continued)

Burst File Name	Source	MJD	DM (pc cm^{-3})	ToA (s)	FWHM (ms)	Bandwidth (MHz)	Peak Flux Density (Jy)	Fluence (Jy ms)
FRB20201124_0069.fits	FRB20201124	59485.78942	412.55	0.6272	4.54	300	0.07142	0.324
FRB20201124_0070.fits	FRB20201124	59485.79069	412.55	1.0980	3.66	300	0.04396	0.161
FRB20201124_0071.fits	FRB20201124	59485.79077	412.55	1.2756	8.3	500	0.06737	0.559
FRB20201124_0072.fits	FRB20201124	59485.79129	412.55	0.6069	6.08	250	0.03764	0.229
FRB20201124_0073.fits	FRB20201124	59485.79462	412.55	4.8612	6.26	250	0.01964	0.123
FRB20201124_0074.fits	FRB20201124	59485.79628	412.55	0.4874	9.4	400	0.16216	1.525
FRB20201124_0075.fits	FRB20201124	59485.79752	412.55	4.1816	6.62	350	0.1511	1.001
FRB20201124_0076.fits	FRB20201124	59485.79845	412.55	1.0572	7.39	300	0.04422	0.327
FRB20201124_0077.fits	FRB20201124	59485.79913	412.55	1.8079	3.97	200	0.02089	0.083
FRB20201124_0078.fits	FRB20201124	59485.80027	412.55	3.6529	4.83	250	0.0623	0.301
FRB20201124_0079.fits	FRB20201124	59485.80083	412.55	0.5508	4.48	350	0.02233	0.1
FRB20201124_0080.fits	FRB20201124	59485.80129	412.55	1.5886	4.06	300	0.03007	0.122
FRB20201124_0081.fits	FRB20201124	59485.80176	412.55	3.4661	6.45	250	0.16727	1.079
FRB20201124_0082.fits	FRB20201124	59485.80197	412.55	2.6063	4	250	0.0885	0.354
FRB20201124_0083.fits	FRB20201124	59485.80202	412.55	0.7513	7.78	300	0.04189	0.326
FRB20201124_0084.fits	FRB20201124	59485.80252	412.55	4.4643	3.65	400	0.04159	0.152
FRB20201124_0085.fits	FRB20201124	59485.8037	412.55	3.9049	7.53	300	0.16536	1.245
FRB20201124_0086.fits	FRB20201124	59485.80449	412.55	0.9515	6.53	450	0.08049	0.526
FRB20201124_0087.fits	FRB20201124	59485.80463	412.55	0.4211	8.51	300	0.06767	0.576
FRB20201124_0088.fits	FRB20201124	59485.80502	412.55	2.0349	7.38	400	0.1015	0.749
FRB20201124_0089.fits	FRB20201124	59485.80516	412.55	1.4380	4.07	400	0.20643	0.84
FRB20201124_0090.fits	FRB20201124	59485.8055	412.55	4.5371	5.49	500	0.09819	0.539
FRB20201124_0091.fits	FRB20201124	59485.80604	412.55	0.4256	2.01	250	0.02288	0.046
FRB20201124_0092.fits	FRB20201124	59485.80673	412.55	0.9239	3.27	200	0.02663	0.087
FRB20201124_0093.fits	FRB20201124	59485.80764	412.55	3.0362	2.89	200	0.05981	0.173
FRB20201124_0094.fits	FRB20201124	59485.8077	412.55	1.6172	6.62	350	0.17298	1.145
FRB20201124_0095.fits	FRB20201124	59485.80853	412.55	2.4244	4.99	200	0.01966	0.098
FRB20201124_0096.fits	FRB20201124	59485.8086	412.55	2.2274	3.46	200	0.02543	0.088
FRB20201124_0097.fits	FRB20201124	59485.8089	412.55	1.9359	7.4	250	0.02379	0.176
FRB20201124_0098.fits	FRB20201124	59485.80898	412.55	2.6103	5.46	200	0.03112	0.17
FRB20201124_0099.fits	FRB20201124	59485.8093	412.55	4.8104	11.69	450	0.14296	1.671
FRB20201124_0100.fits	FRB20201124	59485.80963	412.55	0.9647	4.15	350	0.03327	0.138
FRB20201124_0101.fits	FRB20201124	59485.81049	412.55	3.9232	3.86	500	0.24747	0.955
FRB20201124_0102.fits	FRB20201124	59485.81246	412.55	0.2918	3.8	400	0.26003	0.989
FRB20201124_0103.fits	FRB20201124	59485.81259	412.55	4.9604	5.58	300	0.15388	0.859
FRB20201124_0104.fits	FRB20201124	59485.81263	412.55	2.0772	3.9	150	0.02974	0.116
FRB20201124_0105.fits	FRB20201124	59485.8128	412.55	3.8942	2.16	250	0.02079	0.045
FRB20201124_0106.fits	FRB20201124	59485.81337	412.55	1.9298	3.35	200	0.0421	0.141
FRB20201124_0107.fits	FRB20201124	59485.81412	412.55	1.9697	3.69	400	0.02764	0.102

Table 4 continued

Table 4 (continued)

Burst File Name	Source	MJD	DM (pc cm^{-3})	ToA (s)	FWHM (ms)	Bandwidth (MHz)	Peak Flux Density (Jy)	Fluence (Jy ms)
FRB20201124_0108.fits	FRB20201124	59485.81436	412.55	3.3692	6.72	450	0.18275	1.228
FRB20201124_0109.fits	FRB20201124	59485.81504	412.55	4.2643	2.39	200	0.02221	0.053
FRB20201124_0110.fits	FRB20201124	59485.81517	412.55	2.2309	4.54	500	0.53528	2.43
FRB20201124_0111.fits	FRB20201124	59485.81546	412.55	1.5814	4.78	150	0.01547	0.074
FRB20201124_0112.fits	FRB20201124	59485.8157	412.55	3.4419	8.22	500	0.5477	4.503
FRB20201124_0113.fits	FRB20201124	59485.81594	412.55	4.7306	4.03	400	0.07349	0.296
FRB20201124_0114.fits	FRB20201124	59485.81643	412.55	1.9233	3	350	0.01764	0.053
FRB20201124_0115.fits	FRB20201124	59485.81772	412.55	3.8443	6.21	450	0.09902	0.615
FRB20201124_0116.fits	FRB20201124	59485.81813	412.55	0.6751	5.96	150	0.03457	0.206
FRB20201124_0117.fits	FRB20201124	59485.8182	412.55	0.3228	2.64	150	0.01629	0.043
FRB20201124_0118.fits	FRB20201124	59485.81831	412.55	3.8737	10.91	300	0.05244	0.572
FRB20201124_0119.fits	FRB20201124	59485.81878	412.55	4.8637	7.83	200	0.03536	0.277
FRB20201124_0120.fits	FRB20201124	59485.82044	412.55	0.8118	5.24	450	0.15476	0.811
FRB20201124_0121.fits	FRB20201124	59485.8207	412.55	3.6901	2.67	100	0.02137	0.057
FRB20201124_0122.fits	FRB20201124	59485.82105	412.55	2.1136	4.14	250	0.01377	0.057
FRB20201124_0123.fits	FRB20201124	59485.82185	412.55	0.5208	2.93	200	0.10873	0.319
FRB20201124_0124.fits	FRB20201124	59485.82276	412.55	1.3800	5.01	250	0.03151	0.158
FRB20201124_0125.fits	FRB20201124	59485.82381	412.55	1.8504	4.77	400	0.15554	0.742

REFERENCES

- Agarwal, D., Aggarwal, K., Burke-Spolaor, S., Lorimer, D. R., & Garver-Daniels, N. 2020a, *Monthly Notices of the Royal Astronomical Society*, 497, 1661
- Agarwal, D., Lorimer, D., Surnis, M., et al. 2020b, *Monthly Notices of the Royal Astronomical Society*, 497, 352
- Chen, B. H., Hashimoto, T., Goto, T., et al. 2022, *Monthly Notices of the Royal Astronomical Society*, 509, 1227
- . 2023, *Monthly Notices of the Royal Astronomical Society*, 521, 5738
- Connor, L., & van Leeuwen, J. 2018, *The Astronomical Journal*, 156, 256
- Feng, Y., Li, D., Yang, Y.-P., et al. 2022, *Science*, 375, 1266
- Jiang, P., Yue, Y., Gan, H., et al. 2019, *Science China Physics, Mechanics & Astronomy*, 62, 1
- Jiang, P., Tang, N.-Y., Hou, L.-G., et al. 2020, *Research in Astronomy and Astrophysics*, 20, 064
- Keith, M., Jameson, A., Van Straten, W., et al. 2010, *Monthly Notices of the Royal Astronomical Society*, 409, 619
- Laha, S., Younes, G., Wadiasingh, Z., et al. 2022, *The Astrophysical Journal*, 930, 172
- Li, D., Wang, P., Qian, L., et al. 2018, *IEEE Microwave Magazine*, 19, 112
- Li, D., Wang, P., Zhu, W., et al. 2021, *Nature*, 598, 267
- Liu, Y.-L., Li, J., Liu, Z.-Y., et al. 2022, *Research in Astronomy and Astrophysics*, 22, 105007
- Lorimer, D. 2011, *Astrophysics Source Code Library*, ascl
- Lyon, R. J., Stappers, B., Cooper, S., Brooke, J. M., & Knowles, J. D. 2016, *Monthly Notices of the Royal Astronomical Society*, 459, 1104
- Niu, C.-H., Aggarwal, K., Li, D., et al. 2022a, *Nature*, 606, 873
- Niu, J.-R., Zhu, W.-W., Zhang, B., et al. 2022b, *Research in Astronomy and Astrophysics*, 22, 124004
- Ransom, S. 2011, *Astrophysics source code library*, ascl
- Sanidas, S., Cooper, S., Bassa, C., et al. 2019, *Astronomy & Astrophysics*, 626, A104
- Xu, J., Feng, Y., Li, D., et al. 2023, *Universe*, 9, 330
- Yong, S. Y., Hobbs, G., Huynh, M. T., et al. 2022, *Monthly Notices of the Royal Astronomical Society*, 516, 5832
- Zhang, Y. G., Gajjar, V., Foster, G., et al. 2018, *The Astrophysical Journal*, 866, 149
- Zhang, Y.-K., Li, D., Feng, Y., et al. 2024, arXiv e-prints, arXiv:2410.03200. <https://arxiv.org/abs/2410.03200>
- Zhang, Y.-K., Wang, P., Feng, Y., et al. 2022, *Research in Astronomy and Astrophysics*, 22, 124002